**Title:** Reactive Oxygen Species Regulate Activity-Dependent Neuronal Plasticity in *Drosophila*

**Authors:** Matthew C. W. Oswald[1*], Paul S. Brooks[1], Maarten F. Zwart[2], Amrita Mukherjee[1], Ryan J. H. West[3,4], Carlo Giachello[3], Khomgrit Morarach[1], Richard A. Baines[3], Sean T. Sweeney[4], Matthias Landgraf[1*]

*Correspondence to: mo364@cam.ac.uk and ml10006@cam.ac.uk

**Affiliations:**

[1] University of Cambridge, Department of Zoology, Downing Street, Cambridge, CB2 3EJ, United Kingdom

[2] HHMI Janelia Research Campus, Ashburn, VA, 20147, USA

[3] Faculty of Biology, Medicine and Health, University of Manchester, Oxford Road, Manchester, M13 9PT, UK

[4] Department of Biology, University of York, Heslington York YO10 5DD, United Kingdom

**Abstract:**

Reactive oxygen species (ROS) have been extensively studied as damaging agents associated with ageing and neurodegenerative conditions. Their role in the nervous system under non-pathological conditions has remained poorly understood. Working with the *Drosophila* larval locomotor network, we show that in neurons ROS act as obligate signals required for neuronal activity-dependent structural plasticity, of both pre- and postsynaptic terminals. ROS signaling is also necessary for maintaining evoked synaptic transmission at the neuromuscular junction, and for activity-regulated homeostatic adjustment of motor network output, as measured by larval crawling behavior. We identified the highly conserved Parkinson's disease-linked protein DJ-1ß as a redox sensor in neurons where it regulates structural plasticity, in part via modulation of the PTEN-PI3Kinase pathway. This study provides a new conceptual framework of neuronal ROS as second messengers required for neuronal plasticity and for network tuning, whose dysregulation in the ageing brain and under neurodegenerative conditions may contribute to synaptic dysfunction.

## Introduction

Levels of reactive oxygen species (ROS) in the brain increase with ageing and high levels of ROS are a hallmark of neurodegeneration, including Alzheimer's and Parkinson's disease (Höhn and Grune, 2013; Martins et al., 1986; Spina and Cohen, 1989) for review see (Milton and Sweeney, 2012). Mitochondria are a significant source of ROS, which form as obligate byproducts of respiratory ATP synthesis by 'leakage' of the electron transport chain, thus leading to the generation of superoxide anions ($O_2^-$) and hydrogen peroxide ($H_2O_2$) (Halliwell, 1992). Implicit in their name, ROS are highly reactive, containing one or more unpaired electrons, with the potential to modify and damage by oxidation proteins, lipids and DNA (Gladyshev, 2014; Harman, 1956; Stuart et al., 2014). Importantly, ROS have also been recognized as signaling molecules in metabolic pathways (Liemburg-Apers et al., 2015) and controlling the activity of transcription factors such as AP-1 and Nrf2 (Jindra et al., 2004; Soriano et al., 2009). Moreover, several kinase signaling pathways are enhanced by ROS, either by oxidation of kinase interacting modulators, such as thioredoxin or glutathione-S-transferases (Adler et al., 1999; Saitoh et al., 1998), or through inhibition of counteracting phosphatases, e.g. PTEN, by oxidation of the active site cysteine residue (Finkel, 2011; Stuart et al., 2014; Tonks, 2005).

We previously showed in a model for lysosomal storage diseases that ROS can regulate neuromuscular junction (NMJ) structure (Milton et al., 2011). NMDA receptor stimulation can lead to ROS generation (Bindokas et al., 1996; Brennan et al., 2009; Dugan et al., 1995), and in hippocampal and spinal cord slices ROS have been shown sufficient and necessary for inducing 'Hebbian' forms of plasticity (LTP) (Kamsler and Segal, 2003a; Kamsler and Segal, 2003b; Klann, 1998; Knapp and Klann, 2002; Lee et al., 2010). Conversely, disturbing the ROS balance by over-expression of the scavenger superoxide dismutase caused defects in hippocampal LTP and learning paradigms in mice (Gahtan et al., 1998; Levin et al., 1998; Thiels et al., 2000). Recent studies have linked increased ROS levels with neurodevelopmental conditions such as schizophrenia, bipolar and autism spectrum disorders (Do et al., 2015; Steullet et al., 2017).

Here, we set out to investigate potential roles for ROS in the nervous system under non-pathological conditions, which are much less well understood. The brain is arguably the most energy demanding organ and mitochondrial oxidative phosphorylation is a major source of ROS (Attwell and Laughlin, 2001; Hallermann et al., 2012; Zhu et al., 2012). We therefore asked whether neurons might utilize mitochondrial metabolic ROS as feedback signals to mediate activity-regulated changes. As an experimental model we used the motor system of the fruitfly larva, *Drosophila melanogaster*, which allows access to uniquely identifiable motoneurons in the ventral nerve cord and their specific body wall target muscles (Kohsaka et al., 2012). We established an experimental paradigm for studying activity-regulated structural adjustments across an identified motoneuron, quantifying changes at both pre- and postsynaptic terminals. We show that thermogenetic neuronal over-activation leads to the generation of ROS at presynaptic terminals, and that ROS signaling is necessary and sufficient for the activity-regulated structural adjustments. As a cellular ROS sensor we identified the conserved redox sensitive protein DJ-1ß, a homologue of vertebrate DJ-1 (PARK7) (Meulener et al., 2005), and the phosphatase and tensin homolog (PTEN) and PI3kinase as downstream effectors of activity-ROS-mediated structural plasticity. We find that ROS signaling is

also required for maintaining constancy of evoked transmission at the neuromuscular junction (NMJ) with a separate ROS pathway regulating the amplitude of spontaneous vesicle release events. Behaviourally, ROS signaling is required for the motor network to adjust homeostatically to return to a set crawling speed following prolonged overactivation.

In summary, this study establishes a new framework for studying ROS in the nervous system: as obligatory regulators that inform neurons about their activation status, and as obligatory mediators of activity-induced plasticity, both structural and physiological.

## Results

### Structural plasticity of synaptic terminals is regulated by neuronal activity

Our aim was to explore roles for activity-regulated ROS signaling in the nervous system under non-pathological conditions. Working with the *Drosophila* larval neuromuscular system allowed us to target manipulations to identified nerve cells *in vivo* that manifest structural and functional plasticity (Frank et al., 2013; Tripodi et al., 2008; Wolfram and Baines, 2013; Zwart et al., 2013). We focused on two well characterized motoneurons, 'aCC' and 'RP2', which jointly innervate the dorsal acute muscle 1 (DA1) (Figure 1A) (Baines et al., 1999; Baines et al., 2001; Bate, 1993; Choi et al., 2004; Hoang and Chiba, 2001; Landgraf et al., 2003; Sink and Whitington, 1991). First, we characterized activity-regulated morphological changes at the presynaptic neuromuscular junction (NMJ) and, in the central nervous system (CNS), the branched postsynaptic dendritic arbors that receive input from premotor interneurons (Baines et al., 1999; Schneider-Mizell et al., 2016; Zwart et al., 2013). A simple method for increasing activity in the larval locomotor network is to increase ambient temperature from the default standard of 25$^{o}$C to 29$^{o}$C or 32$^{o}$C. Sigrist et al. (2003) and Zhong and Wu (2004) previously demonstrated this to trigger increased locomotor activity and to result in increased varicosity (bouton) number at presynaptic NMJs (Sigrist et al., 2003; Zhong and Wu, 2004). We were able to reproduce and extend these findings: rearing larvae at higher ambient temperatures results in NMJs having more boutons than controls by the third instar wandering stage, 100 hrs after larval hatching (ALH) (grey data in Figure 1B-C, compare 25$^{o}$C with 29$^{o}$C and 32$^{o}$C conditions). To complement these systemic manipulations and to exclude potential non-specific effects we turned to a cell-specific activation paradigm of selectively overactivating the aCC and RP2 motoneurons via targeted mis-expression of the warmth-gated cation channel dTrpA1. Expression of dTrpA1 in neurons is a well established method for temperature controlled neuronal overactivation (Hamada et al., 2008; Owald et al., 2015). For larval motoneurons in particular, Pulver and colleagues demonstrated that dTrpA1 is activated above 24$^{o}$C, at 25$^{o}$C leading to action potential firing frequencies of 9-12 Hz (moderate activation) and 22-30 Hz at 27$^{o}$C (stronger activation) (Pulver et al., 2009). These activation levels are within the physiological range of larval motoneurons, thought to operate at approximately 42 Hz during muscle contraction cycles (Chouhan et al., 2010). Similar to the systemic manipulations, we found that cell-specific thermogenetic dTrpA1 activation of single motoneurons also led to titratable increases in bouton number at presynaptic NMJs (blue data in Figure 1B-C). Note that these cell-specific dTrpA1-mediated activity manipulations were

carried out at 25°C and 27°C, sufficient to activate dTrpA1 expressing neurons, but otherwise not causing significant changes in NMJ morphology in non-expressing motoneurons (Tsai et al., 2012).

Next, we quantified synapse number at the presynaptic NMJ on muscle DA1, measured by active zones (visualized with the nc82 antibody against the active zone protein Bruchpilot (Wagh et al., 2006)). This describes a more complex relationship. As previously published, a moderate increase in activity, e.g., rearing larvae at 29°C, causes both more boutons and also more active zones to be formed, potentiating transmission at the NMJ (Sigrist et al., 2003). In contrast, further increases in network activity, as effected by rearing larvae at 32°C or by cell-specific dTrpA1-mediated motoneuron activation at increasing temperatures led to progressive active zone reductions (Figure 1D, E).

We then looked at activity-regulated structural changes of the postsynaptic dendritic arbor of the aCC motoneuron, which is known to be plastic during embryonic and larval stages (Hartwig et al., 2008; Tripodi et al., 2008). To this end, we targeted GAL4 and dTrpA1 expression to individual aCC motoneurons (Ou et al., 2008). Morphometric analysis revealed that the size of the aCC postsynaptic dendritic arbor decreased with rising levels of temperature-gated dTrpA1 activity (Figure 1F, G). We and others previously showed that dendritic length of these neurons correlates with input synapse number and synaptic drive (Schneider-Mizell et al., 2016; Zwart et al., 2013).

In summary, we find that the synaptic terminals of larval motoneurons undergo titratable structural changes in response to neuronal overactivation. Postsynaptic dendritic arbor size, and by inference synapse number and synaptic drive (Zwart et al., 2013), negatively correlate with activation levels. At the presynaptic NMJ, synapse number also correlates negatively with activation level - bar a narrow low level activity window that can lead to potentiation (Ataman et al., 2008; Piccioli and Littleton, 2014; Sigrist et al., 2003). Boutons provide an additional anatomical readout for NMJ plasticity, increasing in number with levels of activity. However, no functional significance of bouton number and size has been documented and changes in these bouton parameters are not predictive of changes in synaptic transmission (Campbell and Ganetzky, 2012).

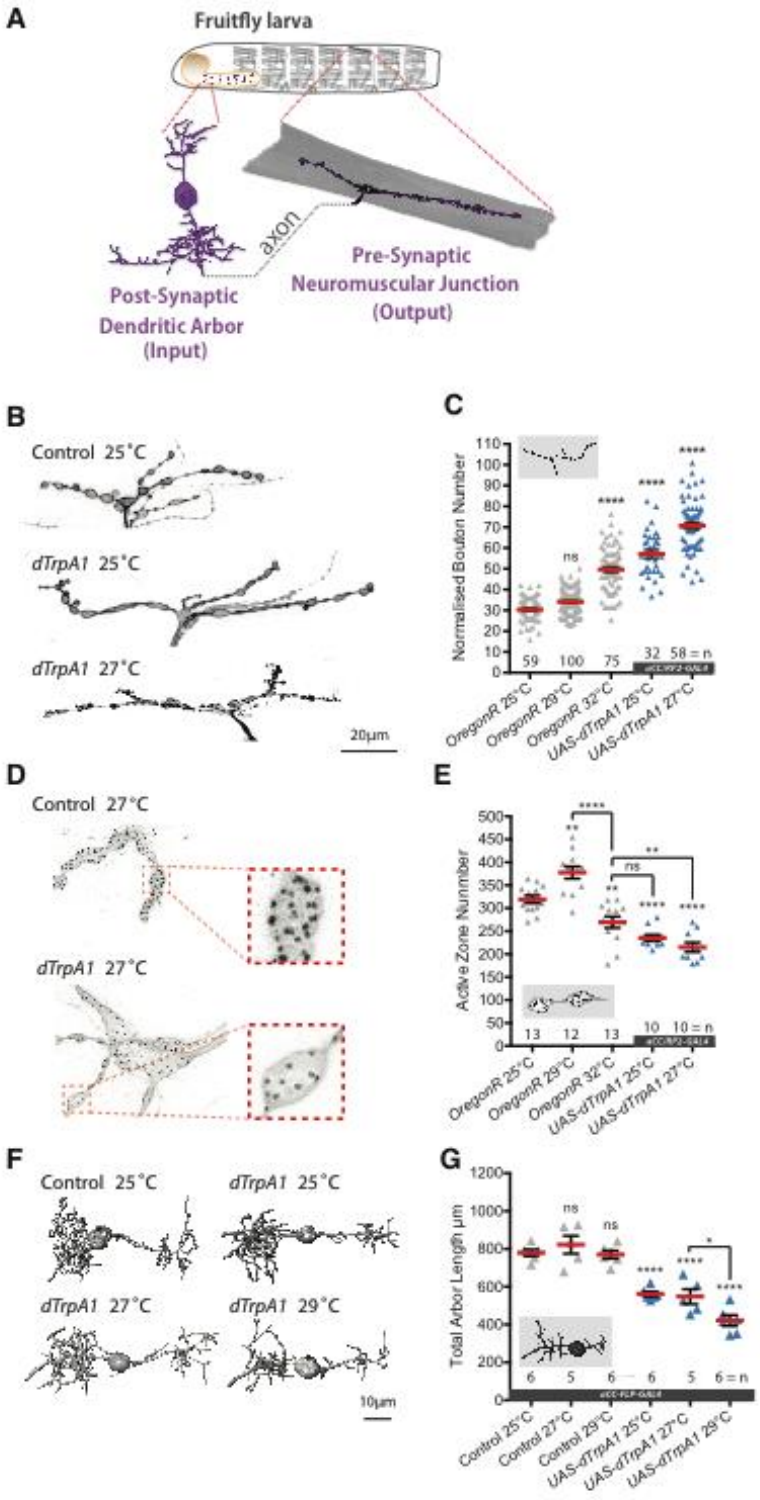


***Figure 1: Adaptive structural synaptic plasticity at motoneuron input and output terminals in response to increased neuronal activity.*** *(**A**) Graphical illustration of a stereotypical larval motoneuron (MN) (adapted from Kohsaka et al. (2012)). Pre-motor interneurons make synaptic connections with the MN dendritic arbor (input) in the larval ventral nerve cord (equivalent of mammalian spinal cord). The MN extends an axonal projection into the periphery where it connects with a target muscle via an NMJ, characterized by varicose swellings (boutons) each containing multiple individual neurotransmitter release sites (active zones). (**B** and **C**) Representative images of*

*muscle DA1 [muscle 1 according to (Crossley, 1978)] NMJs from 3rd instar larvae (100hrs ALH). Dot-plot quantification shows NMJ bouton number increases in response to systemic and cell-specific activity increases. (**D** and **E**) Active zone number increases following low-level overactivation (29°C), but progressively reduces upon stronger overactivation. (**F** and **G**) Digital reconstructions and dot plots show that overactivation leads to reduced total dendritic arbor length of aCC motoneurons (24hrs ALH). 'aCC/RP2-GAL4' expresses GAL4 in all, 'aCC-FLP-GAL4' in single aCC and RP2 motoneurons (see Online Methods for details); 'Control' in (B-G) is heterozygous aCC/RP2-GAL4 or aCC-FLP-GAL4, achieved by crossing the respective GAL4 line to Oregon-R wild type. Mean +/- SEM, ANOVA, ns = not significant, *P<0.05, **P<0.01, ***P<0.001, ****P<0.0001, n = replicate number. Comparisons with control are directly above data points.*

## Neuronal overactivation leads to ROS generation in presynaptic terminals.

Next, we asked if *in vivo* overactivation of individual motoneurons is associated with increased ROS levels, as reported for hippocampal neurons in culture (Hongpaisan et al., 2004). To this end, we co-expressed in aCC and RP2 motoneurons the mitochondrion-targeted ratiometric ROS reporter *UAS-mito-roGFP2-Orp1* (Gutscher et al., 2009) along with *UAS-dTrpA1*. We focused on mitochondria at the muscle DA1 NMJs of wandering third instar larvae (100 hrs ALH). Quantification shows a clear trend of increasing temperature and dTrpA1-mediated activation resulting in progressively greater mean oxidation levels of this ROS sensor in mitochondria at the NMJ (Figure 2A). These data show that *in vivo* dTrpA1-mediated overactivation of *Drosophila* larval motoneurons leads to increased mitochdondrial ROS at presynaptic NMJs.

## Activity generated ROS regulate structural plasticity at synaptic terminals

We then tested whether or not ROS are required for activity-dependent structural synaptic terminal plasticity. To this end we increased neuronal activity in the aCC and RP2 motoneurons via dTrpA1 expression, rearing larvae at 25°C, the lower threshold of dTrpA1 activation that leads to activity-dependent changes of synaptic terminals. At the same time we additionally over-expressed in these neurons ROS scavenging enzymes: Superoxide Dismutase 2 (SOD2), which catalyses $O_2^-$ to $H_2O_2$ reduction; or Catalase, which converts $H_2O_2$ into $H_2O$ and $O_2$. Over-expression of either ROS scavenger enzyme alone showed no effect on NMJ bouton number (Figure 2B). For Catalase over-expression we further quantified active zone number at the NMJ and dendritic arbor size and there too found this indistinguishable from controls (Figure 2C, 3B). In contrast, co-expression of *UAS-Catalase* with *UAS-dTrpA1* significantly counteracted changes in bouton and active zone number otherwise caused by dTrpA1-mediated neuronal overactivation (25°C) (Figure 2B, 3B). Similarly, at the motoneuron input terminals in the CNS, Catalase co-expression rescued dendritic arbor size (Figure 2C). Conversely, SOD2 co-expression enhanced the dTrpA1-mediated increase of bouton number at the NMJ, presumably by potentiating conversion of activity-generated increase of $O_2^-$ into $H_2O_2$ (Figure 2B). We next asked if increasing neuronal ROS was sufficient to invoke structural plasticity in the absence of dTrpA1 activity manipulations. Indeed, cell-specific RNAi knock down of any one of three endogenous ROS scavengers, SOD1, SOD2 or Catalase, led to NMJs with increased bouton number, in agreement with a prior study by Milton et al. (2011), who had demonstrated

oxidative stress causing NMJ growth. These structural NMJ changes are similar to those produced by neuronal overactivation (Figure 2B) and implicate ROS, specifically $H_2O_2$, as a signal for regulating activity-dependent structural plasticity at input and output terminals.

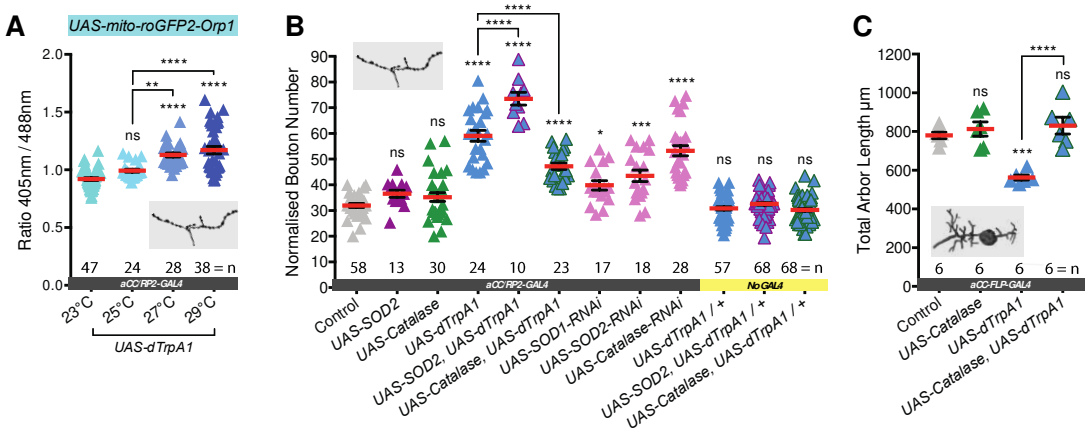


***Figure 2: Neuronal activation leads to generation of synaptic ROS that regulate structural plasticity at input and output terminals.*** *(**A**) Elevated cell-specific activity increases mitochondrial ROS production at NMJs. Dot plots of mitochondrion-targeted ratiometric $H_2O_2$ sensor (UAS-mito-roGFP2-Orp1 (Gutscher et al., 2009)) in wandering 3$^{rd}$ instar larval NMJs (100hrs ALH) at 23˚C (control, dTrpA1 inactive), 25˚C (moderate), 27˚C (strong) and 29˚C (very strong) dTrpA1-mediated overactivation. (**B**) Bouton number at the NMJ is increased by UAS-dTrpA1-mediated overactivation. This is exacerbated by co-expression of UAS-SOD2 (converts $O_2^-$ to $H_2O_2$) and rescued by expression of the $H_2O_2$ scavenger UAS-Catalase. Cell-specific ROS elevation by scavenger knockdown is sufficient to induce NMJ elaboration. aCC/RP2-GAL4, 'Control' is aCC/RP2-GAL4 alone. (**C**) Total dendritic arbor length is reduced by single cell overactivation, but rescued by co-expression of the $H_2O_2$ scavenger UAS-Catalase (aCC motoneurons, 24hr ALH). aCC-FLP-GAL4, 'Control' is aCC-FLP-GAL4 alone, heterozygous, achieved by crossing the GAL4 driver to Oregon-R wild type flies. Larvae were reared at 25°C unless indicated otherwise. Mean +/- SEM, ANOVA, ns = not significant, *P<0.05, **P<0.01, ***P<0.001, ****P<0.0001, n = replicate number.*

## DJ-1ß acts as a ROS sensor in neurons

We then investigated how neurons might sense changes in activity-induced ROS levels. ROS are known to post-translationally modify many different proteins, principally on cysteine or methionine residues, including transcription factors, cytoskeletal proteins, cell adhesion molecules and phosphatases (for review see (Milton and Sweeney, 2012)). We identified DJ-1ß, the fly ortholog of DJ-1 (PARK7), as a candidate ROS sensor. *DJ-1* codes for a highly conserved, ubiquitously expressed redox-sensitive protein, that protects against oxidative stress and regulates mitochondrial function (Ariga et al., 2013; Nagakubo et al., 1997). A mutant allele is also linked to a rare form of familial Parkinsonism (Bonifati et al., 2003). *DJ-1* null mutants are viable without any conspicuous defects and adult flies have been reported to have increased sensitivity to oxidative stress, e.g., as induced by exposure to paraquat or $H_2O_2$ (Meulener et al., 2005). We found that *DJ-1ß* null mutant (*DJ-1ß*$^{\Delta 93}$) larvae develop normally, indistinguishable from wild type controls, and have structurally normal

NMJs (Figure 3A and Figure 3-supplement 1). Interestingly, in larvae homozygous for the *DJ-1ß$^{\Delta 93}$* null mutation, NMJs fail to respond to elevated ROS levels and do not generate additional boutons, as typical for controls when feeding 10mM paraquat, which causes elevated $O_2^-$ release from mitochondrial complex 1, or 10mM Diethyl maleate (DEM), which inactivates the ROS scavenger glutathione (Milton et al., 2011) (Figure 3A). Similarly, loss of DJ-1ß also significantly rescues NMJ bouton addition phenotypes induced by targeted expression of the ROS generator Duox in aCC and RP2 motoneurons, or their dTrpA1-mediated overactivation (Figure 3A). *DJ-1ß$^{\Delta 93}$* mutant larvae also failed to produce the presynaptic bouton and active zone addition that result from raising larvae at 29$^{o}$C (Sigrist et al., 2003) (Figure 3 – supplement 2). The neuronal requirement for *DJ-1ß* was further tested via rescue experiments where neuronal *UAS-DJ-1ß* miss-expression in a *DJ-1ß* null-mutant background proved sufficient to re-establish sensitivity to DEM (see Figure 3 – supplement 3). Next, we cell-autonomously changed the ability of DJ-1ß to act as a redox sensor. DJ-1 is known to form dimers (Lin et al., 2012a). We expressed in aCC and RP2 motoneurons a dominant-acting mutant form of DJ-1ß that is non-oxidizable at the conserved cysteine 104, *UAS-DJ-1ß$^{C104A}$* (Meulener et al., 2006). Expression of DJ-1ß$^{C104A}$ abrogated ROS-induced (following DEM feeding) as well as dTrpA1 activity-mediated NMJ structural adjustment, both with respect to bouton number (Figure 3A) and active zone number (Figure 3B). Looking at activity-dependent structural plasticity of the postsynaptic dendritic arbor, we found this is sensitive to *DJ-1ß* levels; halving the copy number of *DJ-1ß* (in *DJ-1ß$^{\Delta 93}$/+* heterozygotes) was sufficient to significantly suppress dTrpA1-mediated changes to dendritic arbor size (Figure 3C).

In summary, these data show that DJ-1ß is necessary for activity-induced structural changes, compatible with DJ-1ß functioning as a sensor for ROS. DJ-1ß appears to be required in motoneurons for increasing NMJ bouton and active zone numbers in response to mild overactivation regimes that lead to potentiation of transmission at the NMJ (raising larvae at 29$^{o}$C) (Sigrist et al., 2003). At higher levels, as induced by dTrpA1-mediated overactivation, DJ-1ß is also necessary in motoneurons, though under these conditions for decreasing active zone numbers at the NMJ and the size of postsynaptic dendritic arbors.

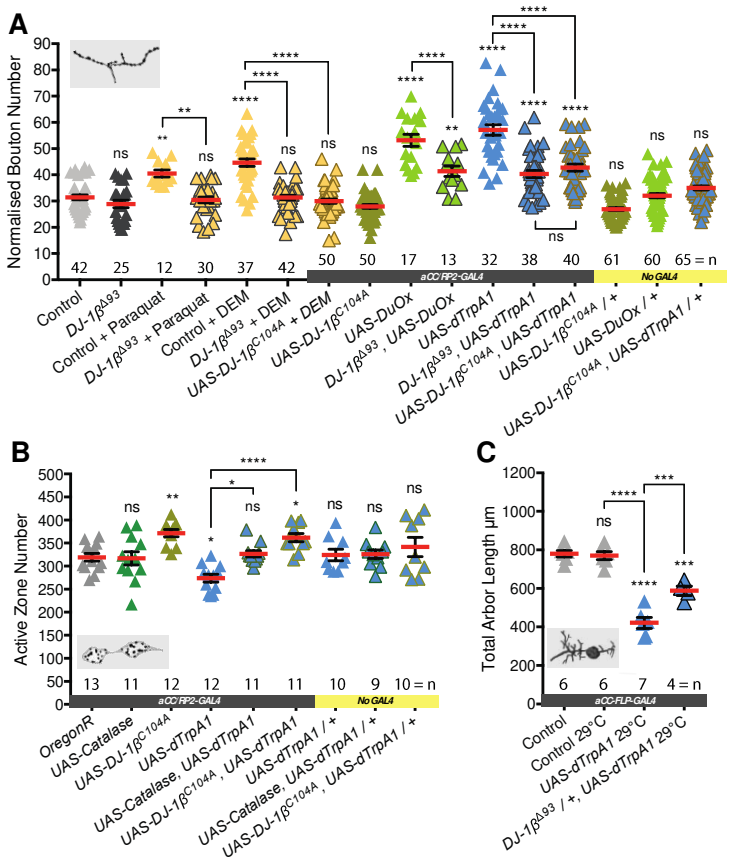


***Figure 3: DJ-1β senses ROS and regulates activity-induced neural plasticity.*** *(**A**) DJ-1β is required for ROS and neuronal-activity-induced NMJ elaboration (100hrs ALH). Larvae reared at 25°C. (**B**) Cell-specific expression of DJ-1β$^{C104A}$, non-oxidizable on conserved cysteine C104, prevents activity-induced reduction of active zone number. 'Control' is aCC/RP2-GAL4 alone. Larvae were reared at 25°C. (**C**) Activity-generated ROS sensing is dose sensitive. Removal of one copy of DJ-1β (in DJ-1β$^{Δ93}$ / + heterozygotes) is sufficient to significantly rescue activity-induced reduction of total dendritic arbor length of motoneurons in 24hr ALH larvae. 'Control' is aCC-FLP-GAL4 alone, heterozygous, achieved by crossing the GAL4 driver to Oregon-R wild type flies.*

## PTEN and PI3K are downstream effectors of the DJ-1ß ROS sensor

Next, we looked for downstream effector pathways responsible for implementing activity and ROS-dependent structural plasticity. DJ-1 is a known redox-regulated inhibitor of PTEN and as such disinhibits PI3Kinase signaling (Kim et al., 2005; Kim et al., 2009b). PI3Kinase was previously shown to regulate bouton and active zone number during NMJ development (Jordán-Álvarez et al., 2012; Martín-Peña et al., 2006). To test if DJ-1ß - PTEN interactions mediate ROS-dependent NMJ adjustments, we performed genetic interaction experiments in the context of DEM-induced ROS elevation (Milton et al., 2011) (Figure 4A). We used different DEM dosages to generate a dose-response curve and focused on changes in NMJ bouton number as a quantitative readout. We found that in controls bouton number increases linearly with exposure to increasing DEM concentrations, peaking at 15mM DEM (Figure 4A). Removal of one copy of *DJ-1ß* (*DJ-1ß$^{Δ93}$/+*) was sufficient to suppress these DEM-induced increases in bouton number. Conversely, removing one copy of the

PI3Kinase antagonist PTEN (*PTEN$^{CO76}$/+*) resulted in increased sensitivity to DEM, as indicated by the left-shifted dose response curve. Larvae made heterozygous mutant for both *DJ-1ß* and *PTEN* (*PTEN$^{CO76}$/+; DJ-1ß$^{\Delta 93}$/+*) were overall less sensitive to DEM than controls, though at higher concentrations displayed greater sensitivity to DEM than *DJ-1ß$^{\Delta 93}$/+* heterozygotes, as might be expected when lowering *PTEN* copy number. These genetic interactions support previous studies (Kim et al., 2005) and complement biochemical data that showed increased binding of DJ-1ß to PTEN following oxidation by $H_2O_2$, thus effecting PTEN inhibition (Kim et al., 2009b).

To further test specificity, we manipulated PTEN and PI3Kinase activities in single cells. Targeted knock-down of endogenous PTEN in aCC and RP2 motoneurons sensitized these to ROS, exacerbating the DEM-induced bouton addition phenotype (Figure 4B). In contrast, over-expression of PTEN or mis-expression of a dominant negative form of PI3Kinase significantly reduced NMJ elaboration normally caused by DEM exposure or dTrpA1-mediated overactivation (Figure 4B). Together these genetic interactions suggest a working model whereby PTEN and PI3Kinase act downstream of DJ-1ß; and neural activity-generated ROS, via oxidation of DJ-1ß, leads to PTEN inhibition. This in turn facilitates a rise in PI3Kinase / $PIP_3$ signaling, which mediates at least part of the structural synaptic terminal plasticity by regulating bouton and active zone number at the NMJ (Figure 7).

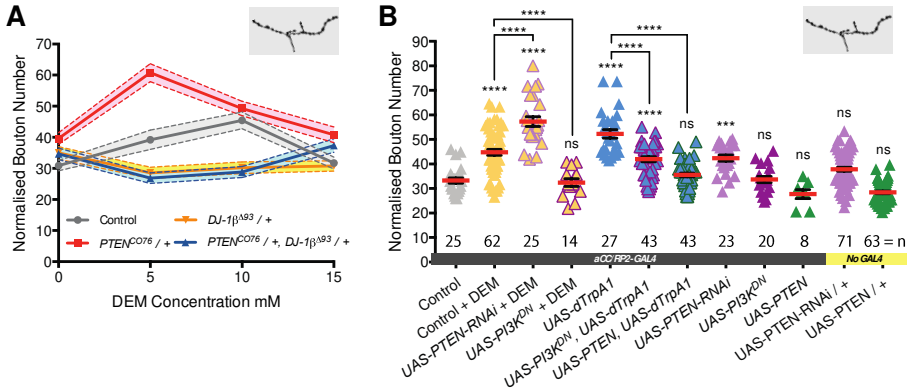


***Figure 4: DJ-1β signals via PTEN and PI3Kinase to regulate ROS and activity-induced NMJ elaboration.*** *(**A**) DJ-1β and PTEN genetically interact to regulate systemic ROS-induced NMJ elaboration. NMJ bouton number varies with ROS (DEM) levels (grey data). Removal of one copy of PTEN sensitizes (red) while heterozygosity for DJ-1ß desensitizes NMJs to ROS levels (yellow), partially restored in double heterozygotes (blue). Dashed boundaries indicate 95 % confidence intervals (n≥38). (**B**) Systemic ROS and activity-induced NMJ structural adjustments require PTEN and PI3Kinase signaling. Over-expression of the PI3Kinase antagonist PTEN or a dominant negative PI3Kinase form abrogates activity-induced NMJ elaboration. 'Control' is aCC/RP2-GAL4 alone, heterozygous, achieved by crossing the GAL4 driver to Oregon-R wild type flies. Mean +/- SEM, ANOVA, ns = not significant, **P<0.01, ***P<0.001, ****P<0.0001, n = replicate number.*

## Activity-regulated ROS signaling is necessary for homeostatic adjustment of synaptic transmission at the NMJ

To complement our studies of structural plasticity at the NMJ, we carried out sharp electrode recordings from the target muscle co-innervated by the aCC and RP2 motoneurons, muscle dorsal

acute 1 (DA1) (Hoang and Chiba, 2001; Landgraf et al., 2003; Mauss et al., 2009). In Oregon-R wild type larvae we recorded evoked excitatory junction potentials (eEJPs) of 18 ±2mV (Figure 5A, D) and miniature excitatory junction potentials (mEJPs) indicative of spontaneous vesicle fusion of 1mV (Figure 5B, D). Therefore, on average each action potential triggers fusion of 18 vesicles at this NMJ (quantal content) (Figure 5C).

We investigated how these parameters of NMJ transmission might change following cell-specific dTrpA1-mediated overactivation of the aCC and RP2 motoneurons (at 25$^{o}$C and 27$^{o}$C). We then tested if these activity-driven changes in transmission required ROS signaling, by co-expressing the ROS scavenger Catalase or by abrogating ROS sensor function through co-expression of the dominant acting, non-oxidizable DJ-1ß variant, DJ-1ß$^{C104A}$. Transmission at NMJs in *Drosophila* is characteristically robust due to several homeostatic regulatory mechanisms working toward maintaining constancy of eEJPs (for reviews see (Frank, 2014; Frank et al., 2013; Harris and Littleton, 2015)). Following dTrpA1-mediated overactivation (rearing larvae at 25$^{o}$C and 27$^{o}$C) evoked NMJ transmission at the muscle DA1 NMJ remains intact and homeostatically balanced (Figure 5A, D). Recordings from controls and larvae with dTrpA1 expressing motoneurons reared at 27$^{o}$C showed noticeably less variability of eEJP amplitude than those made from genetically identical siblings reared at 25$^{o}$C, the dTrpA1 activation threshold, potentially reflecting variable efficacy in motoneuron manipulation (Hamada et al., 2008; Pulver et al., 2009). Overexpression of either Catalase or DJ-1ß$^{C104A}$ has no effect on eEJP amplitude. However, co-expression of Catalase with dTrpA1-mediated overactivation leads to reduction of eEJP amplitude to 7-9mV. This suggests that ROS are required for mechanisms that homeostatically maintain eEJP amplitude (Figure 5A, D).

In contrast, the amplitude of spontaneous vesicle fusion events (mEJP) adjusts inversely with progressively stronger overactivation of motoneurons. These reductions in mEJP amplitude are not specific to dTrpA1-mediated overactivation. Along with others (Ueda and Wu, 2015; Yeates et al., 2017) we also recorded similarly reduced mEJP amplitudes in wild type Oregon-R larvae that had been reared at an elevated temperature (27$^{o}$C *versus* controls reared at 25$^{o}$C) (Figure 5B). Co-expression of DJ-1ß$^{C104A}$ abrogates this activity-dependent reduction of mEJP amplitude (Figure 5B, D), while Catalase co-expression has no effect on mEJP amplitude. Our analysis of quantal content (the mean number of vesicles releasing transmitter per action potential, calculated as the ratio of eEJP/mEJP amplitudes) showed that dTrpA1-mediated motoneuron over-activation at 27 $^{o}$C leads to significantly increased quantal content, and that this is brought back to control levels with co-expression of the $H_2O_2$ scavenger Catalase, as might be expected from the reduced eEJP amplitudes under such conditions.

In summary, evoked transmission at the NMJ is homeostatically maintained despite increased dTrpA1-mediated neuronal overactivation. The maintenance of eEJP amplitude requires ROS and is compromised when the $H_2O_2$ scavenger Catalase is expressed by the presynaptic motoneuron. Activity-regulated changes in mEJP amplitude also depend on ROS signaling, though this is not impacted by the over-expression of cytoplasmic Catalase; instead we found this aspect of synaptic transmission sensitive to oxidation of DJ-1ß.

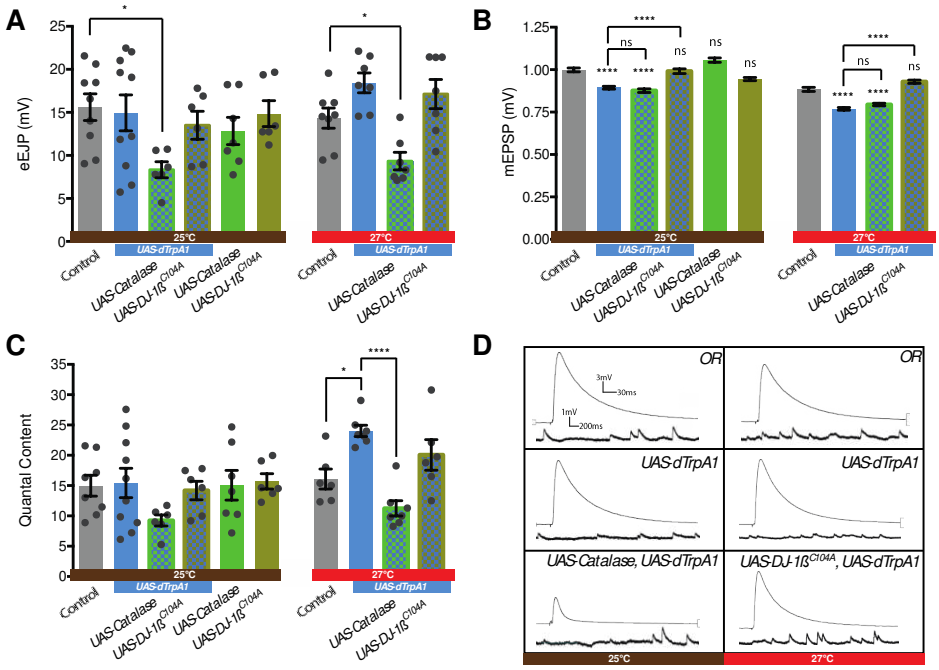


***Figure 5: Pre-synaptic ROS regulate the maintenance of eEJP amplitude and DJ-1ß function is required for the reduction of mEJP amplitude during overactivation.*** *(A) Overactivated motoneurons (expressing dTrpA1 at 25°C, 27°C) show similar eEJP amplitude to control, despite reduced mEJP amplitude (see B). Catalase co-expression prevents this adaptation, significantly reducing eEJP amplitude, whereas DJ-1ß appears not to be required. (B) Increased neuronal activity, mediated by dTrpA1 expression at 25°C or by elevating ambient temperature to 27°C, reduces mEJP amplitude. Co-expression of DJ-1ß$^{C104A}$ rescues this effect. (C) Quantal content (eEJP amplitude / mEJP amplitude) shows no significant difference between groups due to high variance within some conditions. (D) Representative eEJP and mEJP traces. ANOVA, ns = not significant, * P<0.05, **** P<0.0001.*

## Structural plasticity of synaptic terminals is required for homeostatic adjustment of locomotor behavior

We wondered what impact the observed activity-ROS-regulated structural adjustments might have on network output. To test this we used larval crawling speed as a quantifiable readout for a simple locomotor behavior. In agreement with a previous study (Sigrist et al., 2003; Zhong and Wu, 2004), we found that crawling speed increases upon acutely shifting mid-3$^{rd}$ instar larvae (72 hours ALH) to higher ambient temperatures (e.g., from 25°C to 29°C or 32°C) (blue data in Figure 6A). This is to be expected given that these animals have an innate preference for approximately 25$^{o}$C (Dillon et al., 2009; Hamada et al., 2008; Luo et al., 2016; Rosenzweig et al., 2005). In contrast, following prolonged exposure to an elevated temperature, achieved by rearing larvae at 29°C or 32°C, larvae crawled at the same speed characteristic of controls reared at 25°C (average of 0.65 – 0.72mm/second; grey horizontal dotted line in Figure 6A). This crawling speed adaptation is suggestive of a homeostatic adjustment of the locomotor network. Increased network drive might be counteracted by reduced neuronal excitability and/or synaptic input, thus allowing motor output

to be returned to the default crawling speed; in which case one would expect greater adjustment in larvae reared at 32°C than 29°C. To reveal such adjustments we acutely shifted warmth-adapted animals to 25°C, which caused reduced crawling speed (green data in Figure 6A). Indeed, following this downward-shift 32°C-adjusted larvae crawled significantly slower than 29°C-adjusted animals, suggesting the degree of neuronal adjustment is proportional to the level of temperature-induced overactivation. These experiments suggest that during prolonged activity manipulations the larval locomotor network output homeostatically adjusts toward a default crawling speed.

Next, we wanted to test the role of the motoneurons in this form of network adjustment. The motoneurons integrate all pre-motor input within their dendritic arbors and produce the output of the motor network. We targeted expression of dTrpA1 to the motoneurons (and other glutamatergic cells, using *DvGlut-T2A-GAL4*) and reared these animals at 27°C, a temperature that robustly activates dTrpA1-expressing neurons (Hamada et al., 2008; Pulver et al., 2009). Upon acute removal of this overstimulation (by shifting animals to 22°C where the dTrpA1 channel is closed) larval crawling speed reduced significantly relative to non-dTrpA1 expressing controls (Figure 6B). We then asked whether this ROS-mediated structural plasticity of synaptic terminal growth was required for homeostatic adjustment of larval crawling speed, which ensues after prolonged overactivation. We manipulated the ability of neurons to sense increases in ROS levels by targeting expression of the dominant acting non-oxidizable DJ-1ß$^{C104A}$ variant to motoneurons. We then tested the behavior of these animals for adjustment in response to chronic temperature-induced elevation of motor network activity. Our previous set of experiments showed that expression of non-oxidizable DJ-1ß$^{C104A}$ in motoneurons prevents structural adjustment of bouton number and the decrease in active zone number normally caused by overactivation (see Figures 3A & 3B). Expression of non-oxidizable DJ-1ß$^{C104A}$ in motoneurons *per se* did not alter larval crawling speed at the control temperature of 25°C. However, when rearing these larvae at 32°C, which is associated with elevated motor network activation, unlike controls they failed to homeostatically adjust toward the default crawling speed (Figure 6C). Consequently, such larvae reared at elevated temperatures (29°C or 32°C) also responded less strongly than controls to acute temperature downshifts (Figure 6C). These data suggest that activity-induced structural plasticity, implemented through the ROS sensor DJ-1ß, is necessary for activity-directed homeostatic adjustment of larval locomotor behavior.

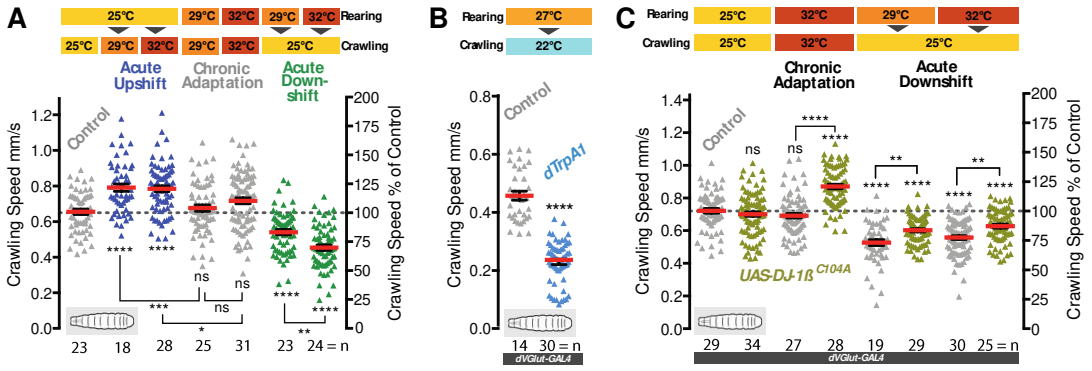


***Figure 6: Adaptive behavioral plasticity in response to chromic locomotor overactivation.*** *(A) Larval motor network activity, assayed by crawling speed 72hrs after larval hatching (AHL), increases*

*in response to acute temperature upshifts (blue) in wild type larvae. In contrast, with prolonged exposure (grey) to elevated temperatures (29°C or 32°C) the motor network adapts homeostatically generating the same crawling speed as 25°C reared controls. This adaptation is further revealed by acute temperature downshifts (green). Each data point represents crawling speed from an individual uninterrupted continuous forward crawl, n = specimen replicate number, up to 3 crawls assayed for each larva. Genotype = OregonR. (**B**) Prolonged overactivation targeted to motoneurons (dVGlut-GAL4; UAS-dTrpA1) also leads to adaptation with reduced crawling speed (dTRPA1 channels open at 27°C, closed at 22°C). Mean +/- SEM, control is dVGlut-GAL4 / +. ****P<0.0001 students t test, n = replicate number. (C) Larvae with expression of UAS-DJ-1$\beta^{C104A}$ targeted to motoneurons (dVGlut-GAL4) are unable to adapt motor network output (crawling speed) to elevated rearing temperatures. Control is dVGlut-GAL4 alone, in heterozygous condition. Each data point represents crawling speed from an individual uninterrupted continuous forward crawl, n = specimen replicate number, up to 3 crawls assayed for each larva. Mean +/- SEM, ANOVA, ns = not significant, *P<0.05, **P<0.01, ***P<0.001, ****P<0.0001.*

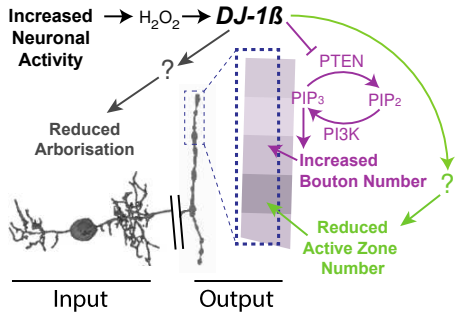


**Figure 7: Model summary**. *DJ-1$\beta$* is a redox signaling hub that coordinates structural synaptic plasticity at motoneuron synaptic input and output terminals. Activity-induced ROS oxidize *DJ-1$\beta$*, leading to PTEN inhibition and thus to a gain in PI3Kinase signaling, which regulates activity-induced NMJ elaboration of boutons and active zones. At higher activity/ROS thresholds additional, yet to be defined, pathways downstream of *DJ-1$\beta$* are activated, implementing adaptive reductions of active zones at the NMJ and dendritic arbor length in the CNS.

## Discussion

### ROS signaling is required for neuronal activity-dependent structural plasticity

Building on previous work that had shown oxidative stress as inducing NMJ growth (Milton et al., 2011), we have in this study identified ROS as obligatory signals for activity-regulated structural plasticity. We further show that ROS are also sufficient to bring about structural changes at synaptic terminals that largely mimic those induced by neuronal overactivation (Figure 2B, C). A mitochondrially targeted ROS reporter (Albrecht et al., 2011; Gutscher et al., 2009) suggests a positive correlation between levels of neuronal activity and ROS generated in mitochondria, potentially as a byproduct of increased ATP metabolism or triggered by mitochondrial calcium influx

(Peng and Jou, 2010) (Figure 2A). Although we did not specifically investigate the nature of the active ROS in this context, three lines of evidence suggest that $H_2O_2$, generated by the dismutation of $O_2^-$, is the principal signaling species. First, under conditions of neuronal overactivation (but not control levels of activity) over-expression of the $O_2^-$ to $H_2O_2$ converting enzyme SOD2 potentiated structural plasticity phenotypes (Figure 2B). Second, over-expression of the $H_2O_2$ scavenger Catalase efficiently counter-acts all activity-induced changes we have quantified, at both postsynaptic dendritic and presynaptic NMJ terminals. Third, over-expression of the $H_2O_2$ generator Duox in motoneurons is sufficient to induce NMJ bouton phenotypes that mimic overactivation (Figure 3A). In addition to mitochondria, other sources of ROS include several oxidases, notably NADPH oxidases. These have been implicated during nervous system development in the regulation of axon growth and synaptic plasticity (Kishida et al., 2006; Munnamalai and Suter, 2009; Munnamalai et al., 2014; Olguín-Albuerne and Morán, 2015; Serrano et al., 2003; Tejada-Simon et al., 2005; Wilson et al., 2016; Wilson et al., 2015). NADPH oxidases can be regulated by NMDA receptor stimulation (Brennan et al., 2009) and activity-associated pathways, including calcium, Protein kinases C and A and calcium/calmodulin-dependent kinase II (CamKII) (Bánfi et al., 2004; Massaad and Klann, 2011; Pandey et al., 2011; Sorce et al., 2017; Tirone and Cox, 2007). The precise sources of activity-regulated ROS, potentially for distinct roles in plasticity, will be interesting to investigate.

## ROS as gatekeepers of activity-dependent synaptic structural plasticity

We demonstrated that ROS are necessary for activity-dependent structural plasticity of *Drosophila* motoneurons, at both their postsynaptic dendrites in the CNS and presynaptic NMJs in the periphery. The mechanisms by which ROS intersect with other known plasticity pathways now need to be investigated. Among well documented signaling pathways regulating synaptic plasticity, are Wnts (Budnik and Salinas, 2011), BMPs (Bayat et al., 2011; Berke et al., 2013), PKA, CREB and the immediate early gene transcription factor AP-1 (Cho et al., 2015; Davis, 2006; Davis and Müller, 2015; Davis et al., 1998; Davis et al., 1996; Kim et al., 2009a; Koles and Budnik, 2012; Osses and Henriquez, 2014; Sanyal et al., 2003; Sanyal et al., 2002; Sulkowski et al., 2014; Walker et al., 2013). ROS signaling could be synergistic with other neuronal plasticity pathways, potentially integrating metabolic feedback. Indeed, ROS modulate BMP signaling in cultured sympathetic neurons (Chandrasekaran et al., 2015) and Wnt pathways in non-neuronal cells (Funato et al., 2006; Love et al., 2013; Rharass et al., 2014). Biochemically, ROS are well known regulators of kinase pathways via oxidation-mediated inhibition of phosphatases (Finkel and Holbrook, 2000; Tonks, 2006). Redox modifications also regulate the activity of the immediate early genes Jun and Fos, which are required for LTP in vertebrates, and in *Drosophila* for activity-dependent plasticity of motoneurons, both at the NMJ and central dendrites (Hartwig et al., 2008; Jindra et al., 2004; Loebrich and Nedivi, 2009; Milton and Sweeney, 2012; Milton et al., 2011; Sanyal et al., 2002). We therefore hypothesize that ROS may provide neuronal activity-regulated modulation of multiple canonical synaptic plasticity pathways.

## Structural plasticity and its coordination between pre- and postsynaptic terminals

We focused on three aspects of synaptic terminal plasticity: dendritic arbor size in the CNS, and bouton and active zone numbers at the NMJ. We used these as phenotypic indicators for activity-regulated changes. By working with identified motoneurons we could observe adaptations across

the entire neuron, relating adjustments of postsynaptic dendritic input terminals in the CNS to changes of the presynaptic output terminals at the NMJ in the periphery. For the aCC motoneuron, the degree of neuronal overactivation correlates with changes in synaptic terminal growth: notably reductions of dendritic arbor size centrally and of active zones at the NMJ. Interestingly, presynaptic active zone numbers did not show a linear response profile. Within a certain range low-level activity increases lead to more active zones, associated with potentiation (as previously shown (Sigrist et al., 2003)); however, with stronger overactivation active zone number decrease (Figure 1D, E). Reduction of active zones, as we observed at the NMJ, and of Brp levels by increased activation was previously also reported in photoreceptor terminals of the *Drosophila* adult visual system (Sugie et al., 2015). At a finer level of resolution it will be interesting to determine how these activity-ROS-mediated structural changes might change active zone cytomatrix composition, which can impact on transmission properties, such as vesicle release probability (Davydova et al., 2014; Lazarevic et al., 2011; Matz et al., 2010; Peled et al., 2014; Weyhersmüller et al., 2011)

We previously found that in these motoneurons dendritic length correlates with the number of input synapses and with synaptic drive (Zwart et al., 2013). Therefore, we tentatively interpret the negative correlation between the degree of overactivation and the reduction in central dendritic arbors as compensatory. In agreement, we found that blockade of activity-induced structural adjustment targeted to the motoneurons prevents behavioral adaptation normally seen after prolonged overactivation (Figure 6). Less clear is if and how overactivation-induced structural changes at the NMJ might be adaptive. Unlike many central synapses that facilitate graded analogue computation, the NMJ is a highly specialized synapse with a large safety factor and intricate mechanisms that ensure constancy of evoked transmission in essentially digital format (Frank et al., 2013; Marrus and DiAntonio, 2005). Rearing larvae at 29$^{o}$C (which acutely increases motor activity) leads to more active zones at the NMJ and potentiated transmission, yet these larvae crawl at the same default speed as other larvae reared at 25$^{o}$C (control) or 32$^{o}$C with reduced numbers of active zones (compare Figure 1E with Figure 6B). This suggests that at least with regard to regulating crawling speed, plasticity mechanisms probably operate at the network level, rather than transmission properties of the NMJ. Indeed, our recordings of transmission at the NMJ, and those reported by others, show homeostatic maintenance of eEJP amplitude irrespective of changes in bouton and active zone number (Figure 5) (Campbell and Ganetzky, 2012). Though in this study we focused on anatomical changes, we expect these structural adjustments to be linked to, and probably preceded by compensatory changes in neuronal excitability that have been documented (Baines et al., 2001; Davis, 2006; Davis et al., 1996; Davis et al., 1998; Driscoll et al., 2013; Frank et al., 2006; Frank et al., 2009; Gaviño et al., 2015; Giachello and Baines, 2016; Lin et al., 2012b; Mee et al., 2004; Müller and Davis, 2012; Wang et al., 2014; Younger et al., 2013; O'Leary et al., 2013; Prinz, 2006; Prinz et al., 2004).

Our observations of activity-regulated adjustments of both dendritic arbor size and NMJ structure give the impression of processes coordinated across the entire neuron. If this was the case, it could be mediated by transcriptional changes, potentially via immediate early genes (AP-1), which are involved in activity and ROS-induced structural changes at the NMJ (Milton et al., 2011; Sanyal et al., 2002) and motoneuron dendrites (Hartwig et al., 2008).

## Identification of DJ-1ß as a neuronal ROS sensor

We discovered that in neurons the highly conserved protein DJ-1ß is critical for both structural and physiological changes in response to activity-generated ROS (Figure 3 and Figure 5). In neurons DJ-1ß might act as a redox sensor for activity-generated ROS. In agreement with this idea, DJ-1ß has been shown to be oxidized by $H_2O_2$ at the conserved cysteine residue C106 (C104 in *Drosophila*) (Lin et al., 2012a; Meulener et al., 2006). Oxidation of DJ-1 leads to changes in DJ-1 function, including translocation from the cytoplasm to the mitochondrial matrix, aiding protection against oxidative damage (Blackinton et al., 2009; Canet-Avilés and Wilson, 2004; Waak et al., 2009) and maintenance of ATP levels (Calì et al., 2015). We found that the ability of motoneurons to respond to increased activation is potently sensitive to DJ-1ß dosage. It is also blocked by expression of mutant DJ-1ß$^{C104A}$ that is non-oxidisable on the conserved Cys104 (Hao et al., 2010; Meulener et al., 2006). These observations suggest that DJ-1ß is critical to ROS sensing in neurons. They also predict that cell type-specific DJ-1ß levels, and associated DJ-1ß reducing mechanisms, could contribute to setting cell type-specific sensitivity thresholds to neuronal activity.

## DJ-1ß downstream pathways implement activity-regulated plasticity

Our data suggest that DJ-1ß could potentially be part of a signaling hub. At the NMJ, this might mediate plasticity across a range, from the addition of active zones associated with potentiation to, following stronger overactivation, the reduction of active zones. We identified disinhibition of PI3Kinase signaling as one DJ-1ß downstream pathway (Figure 4) (Kim et al., 2005; Kim et al., 2009b), a well-studied intermediate in metabolic pathways and a known regulator of synaptic terminal growth, including active zone addition (Jordán-Álvarez et al., 2012; Martín-Peña et al., 2006). However, with stronger overactivation DJ-1ß might engage additional downstream effectors that reduce active zone addition or maintenance, potentially promoting active zone disassembly. While at the presynaptic NMJ PI3Kinase disinhibition explains activity-regulated changes in bouton addition, different DJ-1ß effectors likely operate in the somato-dendritic compartment, which responds to overactivation with reduced growth and possibly pruning (Brierley et al., 2009). Thus, sub-cellular compartmentalization of the activity-ROS-DJ-1ß signaling axis could produce distinct plasticity responses in pre- *versus* postsynaptic terminals.

## Homeostatic maintenance of synaptic transmission requires presynaptic ROS signaling

Previous studies demonstrated a requirement for ROS for LTP (Huddleston et al., 2008; Kamsler and Segal, 2003a; Kamsler and Segal, 2003b; Klann, 1998; Knapp and Klann, 2002; Lee et al., 2010) and found learning defects in animal models with reduced NADPH oxidase activity (Kishida et al., 2006), suggesting that synaptic ROS signaling might be a conserved feature of communication in the nervous system. Our sharp electrode recordings from muscle DA1 revealed three interesting aspects. First, that changing ROS signaling in the presynaptic motoneuron under normal activity conditions does not obviously impact on NMJ transmission. Second, quenching of presynaptic ROS by expression of Catalase under overactivation conditions led to a significant decrease in eEJP

amplitude and concomitantly reduced quantal content (Figure 5A, C). This shows that upon chronic neuronal overactivation ROS signaling is critically required in the presynaptic motoneuron for maintaining eEJP amplitude by increasing vesicle release at the NMJ. This could be achieved by increasing vesicle release probability, which would counteract the reduction in active zone number following a period of neuronal overactivation. In this context it is interesting that components of the presynaptic release machinery, including SNAP25, are thought to be directly modulated by ROS (Giniatullin et al., 2006), while others, such as Complexin, might be indirectly affected, e.g., via ROS-mediated inhibition of phosphatases leading disinhibition of kinase activity (Cho et al., 2015). Third, we found that overactivation of motoneurons leads to reduced mEJP amplitude, also recently reported by others (Yeates et al., 2017). Curiously, mEJP amplitude, unlike eEJP amplitude, is regulated by DJ-1ß, but is not impacted on by artificially increased cytoplasmic levels of the $H_2O_2$ scavenger Catalase. How it is that under conditions of neuronal overactivation eEJP and mEJP amplitudes are differentially sensitive to cytoplasmic Catalase *versus* DJ-1ß oxidation is unclear, though it marks these two processes as distinct. One possibility is that cytoplasmic Catalase changes the local redox status, which could directly affect the properties of the presynaptic active zone cytomatrix. In contrast, mEJP amplitude regulation might be indirect and cell non-autonomous, via modulation of glutamate receptors in the postsynaptic target muscle (Davis et al., 1998). Furthermore, these ROS-regulated adjustments in synaptic transmission are at

Thus, several distinct ROS responsive pathways appear to operate at the NMJ. Structural adjustments in terms of synaptic terminal growth and synapse number are mediated by mechanisms sensitive to DJ-1ß oxidation, potentially regulated via local reducing systems, including Catalase. In addition and distinct from these structural changes, at least in part, are the ROS-regulated adjustments in synaptic transmission that show different ROS sensitivities, one maintaining quantal content of evoked transmission while the other reduces mEJP amplitude when neuronal activity goes up (Figure 5B). It is conceivable that spatially distinct sources of ROS, e.g. mitochondria *versus* membrane localized NADPH oxidases, with different temporal dynamics could potentially mediate such differences in ROS sensitivities at the NMJ.

**Homeostatic adjustment of larval crawling speed depends on redox modification of DJ-1ß**

Our experiments exploring the potential behavioral relevance of activity-regulated structural plasticity demonstrated that network drive is regulated by ambient temperature. Acute elevation in ambient temperature produces faster crawling, while acute temperature reductions have the opposite effect. In contrast, with chronic temperature manipulations, larval crawling returns to its default speed (approx. 0.65 – 0.72mm/sec) (Figure 6A). This adaptation to chronic manipulations might overall be energetically more favorable. It also allows larvae to retain a dynamic range of responses to relative changes in ambient temperature (i.e. speeding up or slowing down).

Where in the locomotor network these adjustments take place remains to be worked out. It is reasonable to assume that proprioceptive sensory neurons, and potentially also central recurrent connections, provide feedback information that facilitates homeostatic adjustment of network output. Our manipulations of the glutamatergic motoneurons show these cells are clearly important. For example, cell type-specific overactivation of the glutamatergic motoneurons (via dTrpA1) on the one hand, and blockade of activity-induced structural adjustment (by mis-expression of non-oxidizable DJ-1ß$^{C104A}$) on the other demonstrated that ROS-DJ-1ß-mediated processes that we

showed important for structural adjustment are also required for implementing homeostatic tuning of locomotor network output (Figure 6B, C). The capacity of motoneurons as important elements in shaping motor network output, might be explicable in that these neurons constitute the final integrators on which all pre-motor inputs converge (Fushiki et al., 2016; Itakura et al., 2015; Kohsaka et al., 2014; Schneider-Mizell et al., 2016; Zwart et al., 2016).

In conclusion, here we identified ROS in neurons as novel signals that are critical for activity-induced structural plasticity. ROS levels regulated by neuronal activity have the potential for operating as metabolic feedback signals. We further identified the conserved redox-sensitive protein DJ-1ß as important to neuronal ROS sensing, and the PTEN/PI3Kinase synaptic growth pathway as a downstream effector pathway for NMJ growth in response to neuronal overactivation. These findings suggest that in the nervous system ROS operate as feedback signals that inform cells about their activity levels. The observation that ROS are important signals for homeostatic processes explains why ROS buffering is comparatively low in neurons (Bell et al., 2015). This view also shines a new light on the potential impact of ROS dysregulation with age or under neurodegenerative conditions, potentially interfering with neuronal adaptive adjustments and thereby contributing to network malfunction and synapse loss.

**Competing interests:** The authors declare that no competing interests exist.

**Acknowledgements:**

We would like to thank Richard Ribchester for invaluable help with setting up a rig for NMJ sharp electrode recording. Nancy Bonini, Tobias Dick, Jörg Grosshans, Karen Hibbard, Fanis Missirlis, Barret Peiffer and Alex Whitworth for generous reagent donations, and Akinao Nose and Hiroshi Kohsaka for kindly helping with figure 1. We would also like to thank Jimena Berni, Alex Whitworth and members of the Landgraf lab for valuable comments on the manuscript. This work was supported by BBSRC research grants (BB/IO1179X/1, BB/M002934/1) to ML and (BB/I012273/1, BB/M002322/1) to STS.

**Materials and Methods**

**Electrophysiology.** Late wandering third instar larvae were fillet dissected in standard HL3 buffer (adapted from (Stewart et al., 1994), 70mM NaCl, 5mM KCl, 20mM $MgCl_2$, 10mM $NaHCO_3$, 115mM Sucrose, 5mM HEPES, 1.5mM CaCl, pH 7.25) ventral surface down with a lateral incision in order preserve both the ventral and dorsal midlines. Suction (GC150F-10 Harvard Apparatus) and sharp

(GC100F-10 Harvard Apparatus) electrodes were pulled using a P-97 pipette puller (Sutter Instrument Company). Sharp electrode muscle impalement (DA1 muscle, at the dorsal midline) and inter-segmental nerve suction (ventral midline) were performed using an Olympus BX50WI compound microscope with 10X air (Olympus 10x/0.25) and 20X dipping (Olympus UMPlanFL 20x/0.5w) objective lenses. Recordings were made at 21°C in HL3 using an Axopatch-1D amplifier (Axon Instruments), a 1322A DigiData (Axon Instruments), a DS2A-MkII Constant Voltage Isolated Stimulator (Digitimer Ltd.) and pCLAMP 10.4 acquisition software (Molecular Devices). mEJP (2-3minutes) and eEJP (3 rounds of 20 stimulations, 5V) recordings were made in current-clamp mode from muscle cells with an input resistance above 8MOhm and a stable resting membrane potential between -40mV and -70mV. Analysis of eEJPs was performed using Clampfit10.6 (Molecular Devices) and mEJPs using Mini-Analysis6.0.7 (Synaptosoft).

**Fly Strains and Husbandry.** Wild-type and transgenic strains were maintained on standard yeast–agar–cornmeal medium at 25 °C. The following fly strains were used: *OregonR* and *PTEN$^{CO76}$* (Bloomington Stock Center, Indiana University), *UAS-dTrpA1* (Hamada et al., 2008), *UAS-SOD2* (Missirlis et al., 2003), *UAS-Catalase* (Missirlis et al., 2001), *UAS-Duox* (Ha, 2005), *DJ-11ß$^{\Delta 93}$* (Meulener et al., 2005), *UAS-DJ-1ß$^{C104A}$* (Meulener et al., 2006), UAS-RNAi lines targeting *SOD1*, *SOD2*, *Catalase* and *PTEN* (KK collection, Vienna Drosophila Resource Centre ) (Dietzl et al., 2007), *UAS-PI3K$^{DN}$* (Leevers et al., 1996), *UAS-PTEN* (Gao et al., 2000). The following two GAL4 expression lines were used to target GAL4 to the aCC and RP2 motoneurons: *aCC-FLP-GAL4* (e*veRN2-Flippase, UAS-myr::mRFP1, UAS-Flp, tubulin84B-FRT-CD2-FRT-GAL4*) (Roy et al., 2007) expresses GAL4 stochastically in single aCC and RP2 motoneurons allowing the imaging of aCC neurons in isolation, as required for dendritic arbor resolution and reconstruction. *aCC/RP2-GAL4* (*eveRN2-GAL4* (Fujioka et al., 2003)*, UAS-myr-mRFP1, UAS-Flp, tubulin84B-FRT-CD2-FRT-GAL4; RRaGAL4, 20xUAS-6XmCherry::HA* (Shearin et al., 2014)) was used for NMJ analysis as it expresses GAL4 in every aCC and RP2 motoneuron. *eveRN2-GAL4* expression is restricted to the embryo and FLPase-gated *tubulin84B-FRT-CD2-FRT-GAL4* maintains GAL4 expression at high levels during larval stages.

**Dissection and Immunocytochemistry**

**1$^{st}$ Instar Ventral Nerve Cord (VNC).** Flies were allowed to lay eggs on apple juice-based agar medium for 24 hrs at 25°C. Embryos were dechorionated using bleach (3.5 minutes room temperature) then incubated (25°C) in pre-warmed Sorensen's saline (pH 7.2, 0.075 M) whilst adhered to a petri dish. Hatched larvae (floating) were recovered hourly and transferred to pre-warmed apple-juice agar plates supplemented with yeast paste. Larvae were allowed to develop for a further 24 hrs (24 hrs after larval hatching, ALH) at 25°C, 27°C or 29°C prior to dissection in Sorensen's saline. A fine hypodermic needle (30 1/2 G; Microlance) was used as a scalpel to cut off the anterior end of each larva, allowing gut, fat body, and trachea to be removed. The ventral nerve chord and brain lobes, extruded with viscera upon decapitation, were dissected out and transferred to a cover glass coated with poly-L-lysine (Sigma-Aldrich), positioned dorsal side up in Sorensen's saline. A clean cover glass was placed on top of the preparation, with strips of double-sided sticky tape as spacers positioned along the edges.

**Wandering 3rd Instar.** Flies were allowed to lay eggs on apple-juice agar based medium overnight at 25°C, larvae were then incubated at 25°C or 27°C until the late wandering 3rd instar stage. Larvae were reared on yeast paste colored with Bromophenol Blue Sodium Salt (Sigma-Aldrich) to allow visualization of gut-clearance, an indicator of the late wandering 3rd instar stage. For Di-ethylmaleate (DEM) (Sigma-Aldrich) and paraquat (Sigma-Aldrich) feeding, yeast paste was made using a 5 mM – 15 mM aqueous solution. Larvae were 'fillet' dissected in Sorensen's saline and fixed for 15 minutes at room temperature in 4% formaldehyde (in Sorenson's saline). Specimens were then washed and stained in Sorensen's saline containing 0.3% Triton X-100 (Sigma-Aldrich) using the following primary / secondary antibodies; Goat-anti-HRP Alexa Fluor 594 (1:400) (Jackson ImmunoResearch Cat. No. 123-585-021), Rabbit-anti-dsRED (1:1200) (ClonTech Cat. No. 632496), Donkey-anti-Rabbit CF568 (1:1200) (Biotium Cat. No. 20098) incubated overnight at 4°C or 2 hrs at room temperature. Specimens were mounted in EverBrite mounting medium (Biotium).

**Image Acquisition and Analysis**

**1st Instar Ventral Nerve Cord (VNC).** Ventral nerve cords were pre-screened for fluorescently labeled, isolated, aCC motoneurons using a Zeiss Axiophot compound epifluorescence microscope and a Zeiss Plan-Neofluar 40x/0.75 N.A. objective lens. Suitable VNCs were imaged immediately with a Yokagawa CSU-22 spinning disk confocal field scanner mounted on an Olympus BX51WI microscope, using a 60×/1.2 N.A. Olympus water immersion objective. Images were acquired with a voxel size of 0.2 × 0.2 × 0.3 µm using a QuantEM cooled EMCCD camera (Photometrics), operated via MetaMorph software (Molecular Devices). Dendritic trees were digitally reconstructed using Amira Resolve RT 4.1 (Visualization Sciences Group and Zuse Institute), supplemented with a 3D reconstruction algorithm (Evers et al., 2005; Schmitt et al., 2004), and images were processed using Amira and ImageJ (National Institutes of Health).

**Wandering 3rd Instar.** Dissected specimens were imaged using a Leica SP5 point-scanning confocal, and a 63x/1.3 N.A. (Leica) glycerol immersion objective lens and LAS AF (Leica Application Suite Advanced Fluorescence) software. Confocal images were processed using ImageJ and Photoshop (Adobe). Bouton number of the NMJ on muscle DA1 [1] from segments A3-A5 was determined by counting every distinct spherical varicosity along the NMJ branch. DA1 muscles were imaged using a Zeiss Axiophot compound microscope and a Zeiss Plan-Neofluar 10x/0.3 N.A. objective lens. Muscle surface area (MSA) was determined by multiplying muscle length by width using ImageJ. In order to correct for subtle differences in animal size (typically 5-10%) bouton number normalization was performed using the following calculation: (mean control MSA / mean experimental MSA) x test bouton number = normalized experimental bouton number.

**Ratiometric ROS Reporter.** *aCC/RP2-Gal4* was used to drive the expression of *UAS-mito-roGFP2-Orp1* (Albrecht et al., 2011; Gutscher et al., 2009) in all aCC and RP2 motoneurons. Wandering third instar larvae were fillet dissected in PBS-NEM (137mM NaCl, 2.7mM KCl, 10mM $Na_2HPO_4$, 1.8mM $KH^2PO_4$, 20mM N-ethylmaleimide (NEM), pH 7.4). Larval fillet preparations were incubated for 5 minutes in PBS-NEM then fixed for 8 minutes in 4% formaldehyde (in PBS-NEM). Specimens were washed three times in PBS-NEM and then equilibrated in 70% glycerol. Specimens were mounted in glycerol and imaged the same day. Imaging was performed on a Leica SP5 point-scanning confocal,

using a 63x/1.3 N.A. (Leica) glycerol immersion objective lens. The reporter was excited sequentially at 405nm and 488nm (Albrecht et al., 2011) with emission detected at 500–535nm. 16-bit images were acquired using Leica LAS AF software and processed using ImageJ. Z-stack images were maximally projected and converted to 32-bit. To remove fringing artefacts around bouton edges 488nm images were thresholded using the 'Intermodes' algorithm with values below threshold set to 'not a number', and ratio images were created by dividing the 405nm image by the 488nm image pixel by pixel (Albrecht et al., 2011). Regions of Interest were taken on the ratio image spanning the entire NMJ and the mean value obtained from each NMJ was used for statistical analysis.

**Transmission Electron Microscopy.** Third instar wandering larvae were fillet dissected in PBS and fixed overnight in 0.1M $NaPO_4$, pH 7.4, 1% glutaraldehyde, and 4% formaldehyde, pH 7.3. Fixed specimens were washed 3× in 0.1M $NaPO_4$ before incubation in $OsO_4$ (1% in 0.1M $NaPO_4$; 2hr). Preparations were washed 3× in distilled water, incubated in 1% uranyl acetate, then washed again (3× distilled water) and dehydrated through a graded ethanol series: 20% increments starting at 30% followed by two 100% changes and then 2× 100% propylene oxide. Specimens were incubated in a graded series of epon araldite resin (in propylene oxide): 25% increments culminating in 3× 100% changes. Individual muscles were then dissected and transferred into embedding molds, followed by polymerization at 60°C for 48 hrs. Resin mounted specimens were sectioned (60–70 nm) using glass knives upon a microtome (Ultracut UCT; Leica). Sections were placed onto grids, incubated in uranyl acetate (50% in ethanol), washed in distilled water and incubated in lead citrate. Sections were imaged using a transmission electron microscope (TECNAI 12 $G^2$; FEI) with a camera (Soft Imaging Solutions MegaView; Olympus) and Tecnai user interface v2.1.8 and analySIS v3.2 (Soft Imaging Systems).

**Behavior – larval crawling analysis**

To record larval crawling, mid-3$^{rd}$ instar larvae (72hrs ALH) were briefly rinsed in water to remove any food and yeast residues, then up to 12 larvae were placed into a 24cm x 24cm arena of 0.8% agar in water, poured to 5 mm thickness. Crawling behavior was recorded in a temperature and humidity controlled incubator at temperatures ranging from 25-32$^{o}$C, as indicated for each experiment. Larvae were allowed to acclimatise for 5 minutes, then recorded for 15 minutes under infrared LED illumination (intensity from 14.33 nW/mm$^2$ in the edge to 9.12 nW/mm$^2$ in the center), using frustrated total internal reflection using a modified FIM tracker (*36*) https://www.uni-muenster.de/PRIA/en/FIM/index.html. Larvae were recorded with a Basler acA2040-180km CMOS camera using Pylon and StreamPix software, mounted with a 16mm KOWA IJM3sHC.SW VIS-NIR Lens. Images were acquired at 5 frames per second. For each larvae, average crawling speed was calculated from long, uninterrupted forward crawls identified manually using FIMTrack. The 15 minute recording period was partitioned into 5 minute sections with each larvae being assayed once within each section, allowing each specimen to be sampled a maximum of 3 times. We observed no change in average crawling speed within the duration of the 15-minute recording.

**Data Analysis.** All data handling was performed using Prism software (GraphPad). NMJ bouton number and ratiometric ROS reporter data were tested for normal / Gaussian distribution using the D'Agostino-Pearson omnibus normality test. Due to a lower replicate number, dendritic arbor

reconstruction data were tested for normality using the Kolmogorov-Smirnov with Dallal-Wilkinson-Lilliefor P value test. Normal distribution was thus confirmed for all data presented, which were compared using one-way analysis of variance (ANOVA), with Tukey's multiple comparisons test where *P<0.05, **P<0.01, ***P<0.001, ****P<0.0001.

## Supplementary Figures

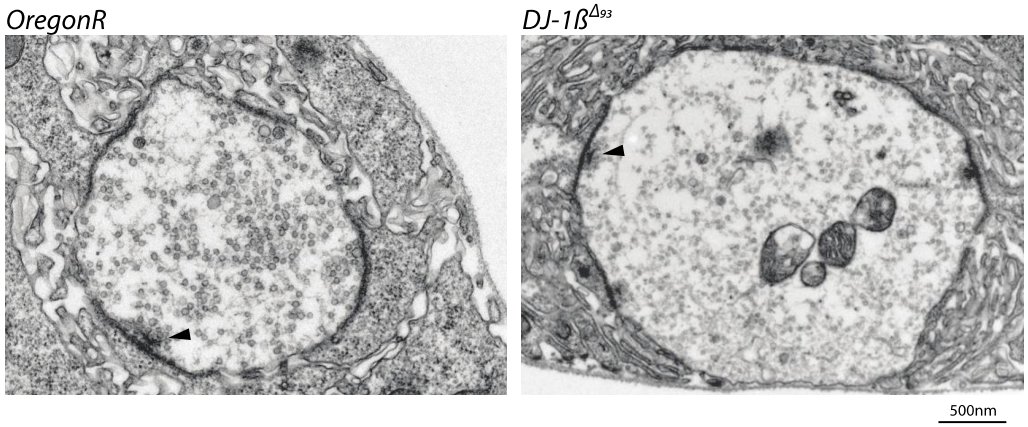


**Figure 3-Figure Supplement 1:** *DJ-1β*$^{\Delta 93}$ mutant 3$^{rd}$ instar larval NMJs are phenotypically normal. Representative TEM bouton cross-sectional images showing that pre-synaptic architecture is intact including active-zones with associated clustered synaptic vesicles (arrowed).

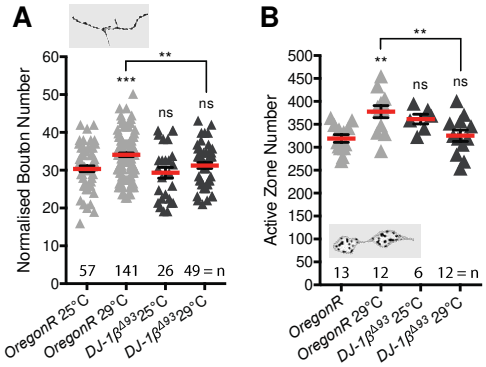


**Figure 3-Figure Supplement 2: A.** *DJ-1β* null mutant (*DJ-1β*$^{\Delta 93}$) larvae do not show systemic activity-dependent NMJ elaboration. Normalised bouton number dot plot showing significantly increased NMJ elaboration in *OregonR*, but not *DJ-1β*$^{\Delta 93}$, larvae reared at 29°C vs 25°C. **B.** *DJ-1β*$^{\Delta 93}$ larvae also do not show systemic activity-dependent increase in active zone number. *OregonR*, but not *DJ-1β*$^{\Delta 93}$, show significantly increased NMJ active zone number when reared at 29°C vs 25°C. Mean +/- SEM, ANOVA **p<0.01, ***p<0.001, n=replicate number.

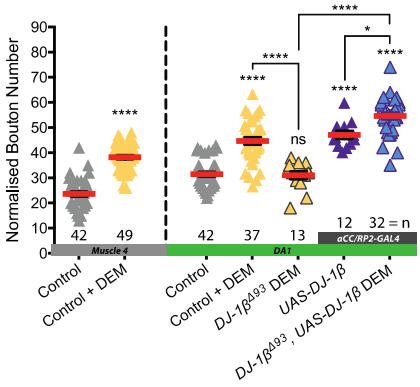


**Figure 3-Figure Supplement 3:** 10mM DEM feeding induces increased bouton number at both muscle 4 and DA1. This response is absent in *DJ-1β* null mutant larvae and is re-established via neuronal (aCC and RP2) specific miss-expression of UAS- *DJ-1β*. UAS- *DJ-1β* expression alone elevates bouton number, which is exacerbated when combined with DEM feeding. Normalised bouton number dot plot, Control is *aCC-FLP-GAL4* alone in heterozygous condition. Mean +/- SEM, ANOVA *p<0.05, ****p<0.0001, n=replicate number.

## References


**Adler, V., Yin, Z., Fuchs, S. Y., Benezra, M., Rosario, L., Tew, K. D., Pincus, M. R., Sardana, M., Henderson, C. J., Wolf, C. R., et al.** (1999). Regulation of JNK signaling by GSTp. *EMBO J* **18**, 1321–1334.

**Albrecht, S. C., Barata, A. G., Grosshans, J., Teleman, A. A. and Dick, T. P.** (2011). In vivo mapping of hydrogen peroxide and oxidized glutathione reveals chemical and regional specificity of redox homeostasis. *Cell Metab* **14**, 819–829.

**Ariga, H., Takahashi-Niki, K., Kato, I., Maita, H., Niki, T. and Iguchi-Ariga, S. M. M.** (2013). Neuroprotective function of DJ-1 in Parkinson's disease. *Oxid Med Cell Longev* **2013**, 683920.

**Ataman, B., Ashley, J., Gorczyca, M., Ramachandran, P., Fouquet, W., Sigrist, S. J. and Budnik, V.** (2008). Rapid activity-dependent modifications in synaptic structure and function require bidirectional Wnt signaling. *Neuron* **57**, 705–718.

**Attwell, D. and Laughlin, S. B.** (2001). An energy budget for signaling in the grey matter of the brain. *J. Cereb. Blood Flow Metab.* **21**, 1133–1145.

**Baines, R. A., Robinson, S. G., Fujioka, M., Jaynes, J. B. and Bate, M.** (1999). Postsynaptic expression of tetanus toxin light chain blocks synaptogenesis in Drosophila. *Curr Biol* **9**, 1267–1270.

**Baines, R. A., Uhler, J. P., Thompson, A., Sweeney, S. T. and Bate, M.** (2001). Altered electrical properties in Drosophila neurons developing without synaptic transmission. *J Neurosci* **21**, 1523–1531.

**Bate, M.** (1993). The mesoderm and its derivatives. In *The Development of Drosophila melanogaster*. (eds. Bate, C. M. and Martinez-Arias, A., Cold Spring Harbor: The development of Drosophila melanogaster.

**Bayat, V., Jaiswal, M. and Bellen, H. J.** (2011). The BMP signaling pathway at the Drosophila neuromuscular junction and its links to neurodegenerative diseases. *Curr Opin Neurobiol* **21**, 182–188.

**Bánfi, B., Tirone, F., Durussel, I., Knisz, J., Moskwa, P., Molnár, G. Z., Krause, K.-H. and Cox, J. A.** (2004). Mechanism of Ca2+ activation of the NADPH oxidase 5 (NOX5). *J Biol Chem* **279**, 18583–18591.

**Bell, K. F. S., Al-Mubarak, B., Martel, M.-A., Mckay, S., Wheelan, N., Hasel, P., Márkus, N. M., Baxter, P., Deighton, R. F., Serio, A., et al.** (2015). Neuronal development is promoted by weakened intrinsic antioxidant defences due to epigenetic repression of Nrf2. *Nat Comms* **6**, 7066.

**Berke, B., Wittnam, J., McNeill, E., Van Vactor, D. L. and Keshishian, H.** (2013). Retrograde BMP signaling at the synapse: a permissive signal for synapse maturation and activity-dependent plasticity. *J Neurosci* **33**, 17937–17950.

**Bindokas, V. P., Jordán, J., Lee, C. C. and Miller, R. J.** (1996). Superoxide production in rat hippocampal neurons: selective imaging with hydroethidine. *J. Neurosci.* **16**, 1324–1336.

**Blackinton, J., Lakshminarasimhan, M., Thomas, K. J., Ahmad, R., Greggio, E., Raza, A. S., Cookson, M. R. and Wilson, M. A.** (2009). Formation of a stabilized cysteine sulfinic acid is critical for the mitochondrial function of the parkinsonism protein DJ-1. *J Biol Chem* **284**, 6476–6485.

**Bonifati, V., Rizzu, P., van Baren, M. J., Schaap, O., Breedveld, G. J., Krieger, E., Dekker, M. C. J., Squitieri, F., Ibanez, P., Joosse, M., et al.** (2003). Mutations in the DJ-1 gene associated with autosomal recessive early-onset parkinsonism. *Science* **299**, 256–259.

**Brennan, A. M., Won Suh, S., Joon Won, S., Narasimhan, P., Kauppinen, T. M., Lee, H., Edling, Y., Chan, P. H. and Swanson, R. A.** (2009). NADPH oxidase is the primary source of superoxide induced by NMDA receptor activation. *Nat Neurosci* **12**, 857–863.

**Brierley, D. J., Blanc, E., Reddy, O. V., VijayRaghavan, K. and Williams, D. W.** (2009). Dendritic targeting in the leg neuropil of Drosophila: the role of midline signalling molecules in generating a myotopic map. *PLoS Biol* **7**, e1000199.

**Budnik, V. and Salinas, P. C.** (2011). Wnt signaling during synaptic development and plasticity. *Curr Opin Neurobiol* **21**, 151–159.

**Calì, T., Ottolini, D., Soriano, M. E. and Brini, M.** (2015). A new split-GFP-based probe reveals DJ-1 translocation into the mitochondrial matrix to sustain ATP synthesis upon nutrient deprivation. *Hum Mol Genet* **24**, 1045–1060.

**Campbell, M. and Ganetzky, B.** (2012). Extensive morphological divergence and rapid evolution of the larval neuromuscular junction in Drosophila. *Proc Natl Acad Sci U S A*.

**Canet-Avilés, R. M. and Wilson, M. A.** (2004). The Parkinson's disease protein DJ-1 is neuroprotective due to cysteine-sulfinic acid-driven mitochondrial localization.

**Chandrasekaran, V., Lea, C., Sosa, J. C., Higgins, D. and Lein, P. J.** (2015). Reactive oxygen species are involved in BMP-induced dendritic growth in cultured rat sympathetic neurons. *Mol Cell Neurosci* **67**, 116–125.

**Cho, R. W., Buhl, L. K., Volfson, D., Tran, A., Li, F., Akbergenova, Y. and Littleton, J. T.** (2015). Phosphorylation of Complexin by PKA Regulates Activity-Dependent Spontaneous Neurotransmitter Release and Structural Synaptic Plasticity. *Neuron* **88**, 749–761.

**Choi, J. C., Park, D. and Griffith, L. C.** (2004). Electrophysiological and morphological characterization of identified motor neurons in the Drosophila third instar larva central nervous system. *J Neurophysiol* **91**, 2353–2365.

**Chouhan, A. K., Zhang, J., Zinsmaier, K. E. and Macleod, G. T.** (2010). Presynaptic mitochondria in functionally different motor neurons exhibit similar affinities for Ca2+ but exert little influence as Ca2+ buffers at nerve firing rates in situ. *J Neurosci* **30**, 1869–1881.

**Crossley, A. C.** (1978). Morphology and development of the Drosophila muscular system. In *Genetics and biology of Drosophila* (eds. Ashburner, M. and Wright, T., pp. 499–560. New York: Genetics and biology of Drosophila.

**Davis, G. W.** (2006). Homeostatic control of neural activity: from phenomenology to molecular design. *Annu Rev Neurosci* **29**, 307–323.

**Davis, G. W. and Müller, M.** (2015). Homeostatic control of presynaptic neurotransmitter release. *Annu Rev Physiol* **77**, 251–270.

**Davis, G. W., DiAntonio, A., Petersen, S. A. and Goodman, C. S.** (1998). Postsynaptic PKA controls quantal size and reveals a retrograde signal that regulates presynaptic transmitter release in Drosophila. *Neuron* **20**, 305–315.

**Davis, G. W., Schuster, C. M. and Goodman, C. S.** (1996). Genetic dissection of structural and functional components of synaptic plasticity. III. CREB is necessary for presynaptic functional plasticity. *Neuron* **17**, 669–679.

**Davydova, D., Marini, C., King, C., Klueva, J., Bischof, F., Romorini, S., Montenegro-Venegas, C., Heine, M., Schneider, R., Schröder, M. S., et al.** (2014). Bassoon specifically controls presynaptic P/Q-type Ca(2+) channels via RIM-binding protein. *Neuron* **82**, 181–194.

**Dietzl, G., Chen, D., Schnorrer, F., Su, K.-C., Barinova, Y., Fellner, M., Gasser, B., Kinsey, K., Oppel, S., Scheiblauer, S., et al.** (2007). A genome-wide transgenic RNAi library for conditional gene inactivation in Drosophila. *Nature* **448**, 151–156.

**Dillon, M. E., Wang, G., Garrity, P. A. and Huey, R. B.** (2009). Review: Thermal preference in Drosophila. *J. Therm. Biol.* **34**, 109–119.

**Do, K. Q., Cuenod, M. and Hensch, T. K.** (2015). Targeting Oxidative Stress and Aberrant Critical Period Plasticity in the Developmental Trajectory to Schizophrenia. *Schizophr Bull* **41**, 835–846.

**Driscoll, H. E., Muraro, N. I., He, M. and Baines, R. A.** (2013). Pumilio-2 regulates translation of nav1.6 to mediate homeostasis of membrane excitability. *J Neurosci* **33**, 9644–9654.

**Dugan, L. L., Sensi, S. L., Canzoniero, L. M., Handran, S. D., Rothman, S. M., Lin, T. S., Goldberg, M. P. and Choi, D. W.** (1995). Mitochondrial production of reactive oxygen species in cortical neurons following exposure to N-methyl-D-aspartate. *J. Neurosci.* **15**, 6377–6388.

**Evers, J. F., Schmitt, S., Sibila, M. and Duch, C.** (2005). Progress in functional neuroanatomy: precise automatic geometric reconstruction of neuronal morphology from confocal image stacks. *J Neurophysiol* **93**, 2331–2342.

**Finkel, T.** (2011). Signal transduction by reactive oxygen species. *J Cell Biol* **194**, 7–15.

**Finkel, T. and Holbrook, N. J.** (2000). Oxidants, oxidative stress and the biology of ageing. *Nature* **408**, 239–247.

**Frank, C. A.** (2014). Homeostatic plasticity at the Drosophila neuromuscular junction. *Neuropharmacology* **78**, 63–74.

**Frank, C. A., Kennedy, M. J., Goold, C. P., Marek, K. W. and Davis, G. W.** (2006). Mechanisms underlying the rapid induction and sustained expression of synaptic homeostasis. *Neuron* **52**, 663–677.

**Frank, C. A., Pielage, J. and Davis, G. W.** (2009). A presynaptic homeostatic signaling system composed of the Eph receptor, ephexin, Cdc42, and CaV2.1 calcium channels. *Neuron* **61**, 556–569.

**Frank, C. A., Wang, X., Collins, C. A., Rodal, A. A., Yuan, Q., Verstreken, P. and Dickman, D. K.** (2013). New approaches for studying synaptic development, function, and plasticity using Drosophila as a model system. *J Neurosci* **33**, 17560–17568.

**Fujioka, M., Lear, B. C., Landgraf, M., Yusibova, G. L., Zhou, J., Riley, K. M., Patel, N. H. and Jaynes, J. B.** (2003). Even-skipped, acting as a repressor, regulates axonal projections in Drosophila. *Development* **130**, 5385–5400.

**Funato, Y., Michiue, T., Asashima, M. and Miki, H.** (2006). The thioredoxin-related redox-regulating protein nucleoredoxin inhibits Wnt-beta-catenin signalling through dishevelled. *Nat Cell Biol* **8**, 501–508.

**Fushiki, A., Zwart, M. F., Kohsaka, H., Fetter, R. D., Cardona, A. and Nose, A.** (2016). A circuit mechanism for the propagation of waves of muscle contraction in Drosophila. *Elife* **5**.

**Gahtan, E., Auerbach, J. M., Groner, Y. and Segal, M.** (1998). Reversible impairment of long-term potentiation in transgenic Cu/Zn-SOD mice. *Eur J Neurosci* **10**, 538–544.

**Gao, X., Neufeld, T. P. and Pan, D.** (2000). Drosophila PTEN regulates cell growth and proliferation through PI3K-dependent and -independent pathways. *Dev Biol* **221**, 404–418.

**Gaviño, M. A., Ford, K. J., Archila, S. and Davis, G. W.** (2015). Homeostatic synaptic depression is achieved through a regulated decrease in presynaptic calcium channel abundance. *Elife* **4**.

**Giachello, C. N. and Baines, R. A.** (2016). Regulation of motoneuron excitability and the setting of homeostatic limits. *Curr Opin Neurobiol* **43**, 1–6.

**Giniatullin, A. R., Darios, F., Shakirzyanova, A., Davletov, B. and Giniatullin, R.** (2006). SNAP25 is a pre-synaptic target for the depressant action of reactive oxygen species on transmitter release. *J Neurochem* **98**, 1789–1797.

**Gladyshev, V. N.** (2014). The free radical theory of aging is dead. Long live the damage theory! *Antioxid Redox Signal* **20**, 727–731.

**Gutscher, M., Sobotta, M. C., Wabnitz, G. H., Ballikaya, S., Meyer, A. J., Samstag, Y. and Dick, T. P.** (2009). Proximity-based protein thiol oxidation by H2O2-scavenging peroxidases. *J Biol Chem* **284**, 31532–31540.

**Ha, E. M.** (2005). A Direct Role for Dual Oxidase in Drosophila Gut Immunity. *Science* **310**, 847–850.

**Hallermann, S., de Kock, C. P. J., Stuart, G. J. and Kole, M. H. P.** (2012). State and location dependence of action potential metabolic cost in cortical pyramidal neurons. *Nat Neurosci* **15**, 1007–1014.

**Halliwell, B.** (1992). Reactive oxygen species and the central nervous system. *J Neurochem* **59**, 1609–1623.

**Hamada, F. N., Rosenzweig, M., Kang, K., Pulver, S. R., Ghezzi, A., Jegla, T. J. and Garrity, P. A.** (2008). An internal thermal sensor controlling temperature preference in Drosophila. *Nature* **454**, 217–220.

**Hao, L.-Y., Giasson, B. I. and Bonini, N. M.** (2010). DJ-1 is critical for mitochondrial function and rescues PINK1 loss of function. *Proc Natl Acad Sci U S A* **107**, 9747–9752.

**HARMAN, D.** (1956). Aging: a theory based on free radical and radiation chemistry. *J Gerontol* **11**, 298–300.

**Harris, K. P. and Littleton, J. T.** (2015). Transmission, Development, and Plasticity of Synapses. *Genetics* **201**, 345–375.

**Hartwig, C. L., Worrell, J., Levine, R. B., Ramaswami, M. and Sanyal, S.** (2008). Normal dendrite growth in Drosophila motor neurons requires the AP-1 transcription factor. *Dev Neurobiol* **68**, 1225–1242.

**Hoang, B. and Chiba, A.** (2001). Single-cell analysis of Drosophila larval neuromuscular synapses. *Dev Biol* **229**, 55–70.

**Hongpaisan, J., Winters, C. A. and Andrews, S. B.** (2004). Strong calcium entry activates mitochondrial superoxide generation, upregulating kinase signaling in hippocampal neurons. *J Neurosci* **24**, 10878–10887.

**Höhn, A. and Grune, T.** (2013). Lipofuscin: formation, effects and role of macroautophagy. *Redox Biol* **1**, 140–144.

**Huddleston, A. T., Tang, W., Takeshima, H., Hamilton, S. L. and Klann, E.** (2008). Superoxide-induced potentiation in the hippocampus requires activation of ryanodine receptor type 3 and ERK. *J Neurophysiol* **99**, 1565–1571.

**Itakura, Y., Kohsaka, H., Ohyama, T., Zlatic, M., Pulver, S. R. and Nose, A.** (2015). Identification of Inhibitory Premotor Interneurons Activated at a Late Phase in a Motor Cycle during Drosophila Larval Locomotion. *PLoS ONE* **10**, e0136660.

**Jindra, M., Gaziova, I., Uhlirova, M., Okabe, M., Hiromi, Y. and Hirose, S.** (2004). Coactivator MBF1 preserves the redox-dependent AP-1 activity during oxidative stress in Drosophila. *EMBO J* **23**, 3538–3547.

**Jordán-Álvarez, S., Fouquet, W., Sigrist, S. J. and Acebes, A.** (2012). Presynaptic PI3K activity triggers the formation of glutamate receptors at neuromuscular terminals of Drosophila. *J Cell Sci* **125**, 3621–3629.

**Kamsler, A. and Segal, M.** (2003a). Hydrogen peroxide modulation of synaptic plasticity. *J Neurosci* **23**, 269–276.

**Kamsler, A. and Segal, M.** (2003b). Paradoxical actions of hydrogen peroxide on long-term potentiation in transgenic superoxide dismutase-1 mice. *J Neurosci* **23**, 10359–10367.

**Kim, R. H., Peters, M., Jang, Y., Shi, W., Pintilie, M., Fletcher, G. C., DeLuca, C., Liepa, J., Zhou, L., Snow, B., et al.** (2005). DJ-1, a novel regulator of the tumor suppressor PTEN. *Cancer Cell* **7**, 263–273.

**Kim, S. M., Kumar, V., Lin, Y. Q., Karunanithi, S. and Ramaswami, M.** (2009a). Fos and Jun potentiate individual release sites and mobilize the reserve synaptic vesicle pool at the Drosophila larval motor synapse. *Proc Natl Acad Sci U S A* **106**, 4000–4005.

**Kim, Y.-C., Kitaura, H., Taira, T., Iguchi-Ariga, S. M. M. and Ariga, H.** (2009b). Oxidation of DJ-1-dependent cell transformation through direct binding of DJ-1 to PTEN. *Int J Oncol* **35**, 1331–1341.

**Kishida, K. T., Hoeffer, C. A., Hu, D., Pao, M., Holland, S. M. and Klann, E.** (2006). Synaptic plasticity deficits and mild memory impairments in mouse models of chronic granulomatous disease. *Mol Cell Biol* **26**, 5908–5920.

**Klann, E.** (1998). Cell-permeable scavengers of superoxide prevent long-term potentiation in hippocampal area CA1. *J Neurophysiol* **80**, 452–457.

**Knapp, L. T. and Klann, E.** (2002). Potentiation of hippocampal synaptic transmission by superoxide requires the oxidative activation of protein kinase C. *J Neurosci* **22**, 674–683.

**Kohsaka, H., Okusawa, S., Itakura, Y., Fushiki, A. and Nose, A.** (2012). Development of larval motor circuits in Drosophila. *Dev Growth Differ* **54**, 408–419.

**Kohsaka, H., Takasu, E., Morimoto, T. and Nose, A.** (2014). A group of segmental premotor interneurons regulates the speed of axial locomotion in Drosophila larvae. *Curr Biol* **24**, 2632–2642.

**Koles, K. and Budnik, V.** (2012). Wnt signaling in neuromuscular junction development. *Cold Spring Harb Perspect Biol* **4**.

**Landgraf, M., Jeffrey, V., Fujioka, M., Jaynes, J. B. and Bate, M.** (2003). Embryonic origins of a motor system: motor dendrites form a myotopic map in Drosophila. *PLoS Biol* **1**, E41.

**Lazarevic, V., Schöne, C., Heine, M., Gundelfinger, E. D. and Fejtova, A.** (2011). Extensive remodeling of the presynaptic cytomatrix upon homeostatic adaptation to network activity silencing. *J Neurosci* **31**, 10189–10200.

**Lee, K. Y., Chung, K. and Chung, J. M.** (2010). Involvement of reactive oxygen species in long-term potentiation in the spinal cord dorsal horn. *J Neurophysiol* **103**, 382–391.

**Leevers, S. J., Weinkove, D., MacDougall, L. K., Hafen, E. and Waterfield, M. D.** (1996). The Drosophila phosphoinositide 3-kinase Dp110 promotes cell growth. *EMBO J* **15**, 6584–6594.

**Levin, E. D., Brady, T. C., Hochrein, E. C., Oury, T. D., Jonsson, L. M., Marklund, S. L. and Crapo, J. D.** (1998). Molecular manipulations of extracellular superoxide dismutase: functional importance for learning. *Behav. Genet.* **28**, 381–390.

**Liemburg-Apers, D. C., Willems, P. H. G. M., Koopman, W. J. H. and Grefte, S.** (2015). Interactions between mitochondrial reactive oxygen species and cellular glucose metabolism. *Arch. Toxicol.* **89**, 1209–1226.

**Lin, J., Prahlad, J. and Wilson, M. A.** (2012a). Conservation of oxidative protein stabilization in an insect homologue of parkinsonism-associated protein DJ-1. *Biochemistry* **51**, 3799–3807.

**Lin, W.-H., Günay, C., Marley, R., Prinz, A. A. and Baines, R. A.** (2012b). Activity-dependent alternative splicing increases persistent sodium current and promotes seizure. *J Neurosci* **32**, 7267–7277.

**Loebrich, S. and Nedivi, E.** (2009). The function of activity-regulated genes in the nervous system. *Physiol Rev* **89**, 1079–1103.

**Love, N. R., Chen, Y., Ishibashi, S., Kritsiligkou, P., Lea, R., Koh, Y., Gallop, J. L., Dorey, K. and Amaya, E.** (2013). Amputation-induced reactive oxygen species are required for successful Xenopus tadpole tail regeneration. *Nat Cell Biol*.

**Luo, J., Shen, W. L. and Montell, C.** (2016). TRPA1 mediates sensation of the rate of temperature change in Drosophila larvae. *Nat Neurosci*.

**Marrus, S. B. and DiAntonio, A.** (2005). Investigating the safety factor at an invertebrate neuromuscular junction. *J Neurobiol* **63**, 62–69.

**Martins, R. N., Harper, C. G., Stokes, G. B. and Masters, C. L.** (1986). Increased cerebral glucose-6-phosphate dehydrogenase activity in Alzheimer's disease may reflect oxidative stress. *J Neurochem* **46**, 1042–1045.

**Martín-Peña, A., Acebes, A., Rodríguez, J.-R., Sorribes, A., de Polavieja, G. G., Fernández-Fúnez, P. and Ferrús, A.** (2006). Age-independent synaptogenesis by phosphoinositide 3 kinase. *J Neurosci* **26**, 10199–10208.

**Massaad, C. A. and Klann, E.** (2011). Reactive oxygen species in the regulation of synaptic plasticity and memory. *Antioxid Redox Signal* **14**, 2013–2054.

**Matz, J., Gilyan, A., Kolar, A., McCarvill, T. and Krueger, S. R.** (2010). Rapid structural alterations of the active zone lead to sustained changes in neurotransmitter release. *Proc Natl Acad Sci U S A* **107**, 8836–8841.

**Mauss, A., Tripodi, M., Evers, J. F. and Landgraf, M.** (2009). Midline signalling systems direct the formation of a neural map by dendritic targeting in the Drosophila motor system. *PLoS Biol* **7**, e1000200.

**Mee, C. J., Pym, E. C. G., Moffat, K. G. and Baines, R. A.** (2004). Regulation of neuronal excitability through pumilio-dependent control of a sodium channel gene. *J Neurosci* **24**, 8695–8703.

**Meulener, M. C., Xu, K., Thomson, L., Thompson, L., Ischiropoulos, H. and Bonini, N. M.** (2006). Mutational analysis of DJ-1 in Drosophila implicates functional inactivation by oxidative damage and aging. *Proc Natl Acad Sci USA* **103**, 12517–12522.

**Meulener, M., Whitworth, A. J., Armstrong-Gold, C. E., Rizzu, P., Heutink, P., Wes, P. D., Pallanck, L. J. and Bonini, N. M.** (2005). Drosophila DJ-1 mutants are selectively sensitive to environmental toxins associated with Parkinson's disease. *Curr Biol* **15**, 1572–1577.

**Milton, V. J. and Sweeney, S. T.** (2012). Oxidative stress in synapse development and function. *Dev Neurobiol* **72**, 100–110.

**Milton, V. J., Jarrett, H. E., Gowers, K., Chalak, S., Briggs, L., Robinson, I. M. and Sweeney, S. T.** (2011). Oxidative stress induces overgrowth of the Drosophila neuromuscular junction. *Proc Natl Acad Sci U S A* **108**, 17521–17526.

**Missirlis, F., Phillips, J. P. and Jäckle, H.** (2001). Cooperative action of antioxidant defense systems in Drosophila. *Current Biology* **11**, 1272–1277.

**Missirlis, F., Rahlfs, S., Dimopoulos, N., Bauer, H., Becker, K., Hilliker, A., Phillips, J. P. and Jäckle, H.** (2003). A putative glutathione peroxidase of Drosophila encodes a thioredoxin peroxidase that provides resistance against oxidative stress but fails to complement a lack of catalase activity. *Biol Chem* **384**, 463–472.

**Munnamalai, V. and Suter, D. M.** (2009). Reactive oxygen species regulate F-actin dynamics in neuronal growth cones and neurite outgrowth. *J Neurochem* **108**, 644–661.

**Munnamalai, V., Weaver, C. J., Weisheit, C. E., Venkatraman, P., Agim, Z. S., Quinn, M. T. and Suter, D. M.** (2014). Bidirectional interactions between NOX2-type NADPH oxidase and the F-actin cytoskeleton in neuronal growth cones. *J Neurochem* **130**, 526–540.

**Müller, M. and Davis, G. W.** (2012). Transsynaptic control of presynaptic $Ca^{2+}$ influx achieves homeostatic potentiation of neurotransmitter release. *Curr Biol* **22**, 1102–1108.

**Nagakubo, D., Taira, T., Kitaura, H., Ikeda, M., Tamai, K., Iguchi-Ariga, S. M. and Ariga, H.** (1997). DJ-1, a novel oncogene which transforms mouse NIH3T3 cells in cooperation with ras. *Biochem Biophys Res Commun* **231**, 509–513.

**O'Leary, T., Williams, A. H., Caplan, J. S. and Marder, E.** (2013). Correlations in ion channel expression emerge from homeostatic tuning rules. *Proc Natl Acad Sci U S A* **110**, E2645–54.

**Olguín-Albuerne, M. and Morán, J.** (2015). ROS produced by NOX2 control in vitro development of cerebellar granule neurons development. *ASN Neuro* **7**.

**Osses, N. and Henriquez, J. P.** (2014). Bone morphogenetic protein signaling in vertebrate motor neurons and neuromuscular communication. *Front Cell Neurosci* **8**, 453.

**Ou, Y., Chwalla, B., Landgraf, M. and van Meyel, D. J.** (2008). Identification of genes influencing dendrite morphogenesis in developing peripheral sensory and central motor neurons. *Neural development* **3**, 16.

**Owald, D., Lin, S. and Waddell, S.** (2015). Light, heat, action: neural control of fruit fly behaviour. *Philos Trans R Soc Lond, B, Biol Sci* **370**, 20140211.

**Pandey, D., Gratton, J.-P., Rafikov, R., Black, S. M. and Fulton, D. J. R.** (2011). Calcium/calmodulin-dependent kinase II mediates the phosphorylation and activation of NADPH oxidase 5. *Mol. Pharmacol.* **80**, 407–415.

**Peled, E. S., Newman, Z. L. and Isacoff, E. Y.** (2014). Evoked and spontaneous transmission favored by distinct sets of synapses. *Curr Biol* **24**, 484–493.

**Peng, T.-I. and Jou, M.-J.** (2010). Oxidative stress caused by mitochondrial calcium overload. *Ann N Y Acad Sci* **1201**, 183–188.

**Piccioli, Z. D. and Littleton, J. T.** (2014). Retrograde BMP Signaling Modulates Rapid Activity-Dependent Synaptic Growth via Presynaptic LIM Kinase Regulation of Cofilin. *J Neurosci* **34**, 4371–4381.

**Prinz, A. A.** (2006). Insights from models of rhythmic motor systems. *Curr Opin Neurobiol* **16**, 615–620.

**Prinz, A. A., Bucher, D. and Marder, E.** (2004). Similar network activity from disparate circuit parameters. *Nat Neurosci* **7**, 1345–1352.

**Pulver, S. R., Pashkovski, S. L., Hornstein, N. J., Garrity, P. A. and Griffith, L. C.** (2009). Temporal dynamics of neuronal activation by Channelrhodopsin-2 and TRPA1 determine behavioral output in Drosophila larvae. *J Neurophysiol* **101**, 3075–3088.

**Rharass, T., Lemcke, H., Lantow, M., Kuznetsov, S. A., Weiss, D. G. and Panáková, D.** (2014). Ca2+-mediated mitochondrial reactive oxygen species metabolism augments Wnt/β-catenin pathway activation to facilitate cell differentiation. *J Biol Chem* **289**, 27937–27951.

**Rosenzweig, M., Brennan, K. M., Tayler, T. D., Phelps, P. O., Patapoutian, A. and Garrity, P. A.** (2005). The Drosophila ortholog of vertebrate TRPA1 regulates thermotaxis. *Genes Dev* **19**, 419–424.

**Roy, B., Singh, A. P., Shetty, C., Chaudhary, V., North, A., Landgraf, M., VijayRaghavan, K. and Rodrigues, V.** (2007). Metamorphosis of an identified serotonergic neuron in the Drosophila olfactory system. *Neural development* **2**, 20.

**Saitoh, M., Nishitoh, H., Fujii, M., Takeda, K., Tobiume, K., Sawada, Y., Kawabata, M., Miyazono, K. and Ichijo, H.** (1998). Mammalian thioredoxin is a direct inhibitor of apoptosis signal-regulating kinase (ASK) 1. *EMBO J* **17**, 2596–2606.

**Sanyal, S., Narayanan, R., Consoulas, C. and Ramaswami, M.** (2003). Evidence for cell autonomous AP1 function in regulation of Drosophila motor-neuron plasticity. *BMC neuroscience* **4**, 20.

**Sanyal, S., Sandstrom, D. J., Hoeffer, C. A. and Ramaswami, M.** (2002). AP-1 functions upstream of CREB to control synaptic plasticity in Drosophila. *Nature* **416**, 870–874.

**Schmitt, S., Evers, J. F., Duch, C., Scholz, M. and Obermayer, K.** (2004). New methods for the computer-assisted 3-D reconstruction of neurons from confocal image stacks. *Neuroimage* **23**, 1283–1298.

**Schneider-Mizell, C. M., Gerhard, S., Longair, M., Kazimiers, T., Li, F., Zwart, M. F., Champion, A., Midgley, F. M., Fetter, R. D., Saalfeld, S., et al.** (2016). Quantitative neuroanatomy for connectomics in Drosophila. *Elife* **5**.

**Serrano, F., Kolluri, N. S., Wientjes, F. B., Card, J. P. and Klann, E.** (2003). NADPH oxidase immunoreactivity in the mouse brain. *Brain Res* **988**, 193–198.

**Shearin, H. K., Macdonald, I. S., Spector, L. P. and Stowers, R. S.** (2014). Hexameric GFP and mCherry Reporters for the Drosophila GAL4, Q, and LexA Transcription Systems. *Genetics* **196**, 951–960.

**Sigrist, S. J., Reiff, D. F., Thiel, P. R., Steinert, J. R. and Schuster, C. M.** (2003). Experience-dependent strengthening of Drosophila neuromuscular junctions. *J Neurosci* **23**, 6546–6556.

**Sink, H. and Whitington, P. M.** (1991). Location and connectivity of abdominal motoneurons in the embryo and larva of Drosophila melanogaster. *J Neurobiol* **22**, 298–311.

**Sorce, S., Stocker, R., Seredenina, T., Holmdahl, R., Aguzzi, A., Chio, A., Depaulis, A., Heitz, F., Olofsson, P., Olsson, T., et al.** (2017). NADPH oxidases as drug targets and biomarkers in neurodegenerative diseases: What is the evidence? *Free Radic Biol Med* **112**, 387–396.

**Soriano, F. X., Baxter, P., Murray, L. M., Sporn, M. B., Gillingwater, T. H. and Hardingham, G. E.** (2009). Transcriptional regulation of the AP-1 and Nrf2 target gene sulfiredoxin. *Mol. Cells* **27**, 279–282.

**Spina, M. B. and Cohen, G.** (1989). Dopamine turnover and glutathione oxidation: implications for Parkinson disease. *Proc Natl Acad Sci USA* **86**, 1398–1400.

**Steullet, P., Cabungcal, J.-H., Coyle, J., Didriksen, M., Gill, K., Grace, A. A., Hensch, T. K., LaMantia, A.-S., Lindemann, L., Maynard, T. M., et al.** (2017). Oxidative stress-driven parvalbumin interneuron impairment as a common mechanism in models of schizophrenia. *Mol. Psychiatry* **22**, 936–943.

**Stewart, B. A., Atwood, H. L., Renger, J. J., Wang, J. and Wu, C. F.** (1994). Improved stability of Drosophila larval neuromuscular preparations in haemolymph-like physiological solutions. *J Comp Physiol A* **175**, 179–191.

**Stuart, J. A., Maddalena, L. A., Merilovich, M. and Robb, E. L.** (2014). A midlife crisis for the mitochondrial free radical theory of aging. *Longev Healthspan* **3**, 4.

**Sugie, A., Hakeda-Suzuki, S., Suzuki, E., Silies, M., Shimozono, M., Möhl, C., Suzuki, T. and Tavosanis, G.** (2015). Molecular Remodeling of the Presynaptic Active Zone of Drosophila Photoreceptors via Activity-Dependent Feedback. *Neuron* **86**, 711–725.

**Sulkowski, M., Kim, Y.-J. and Serpe, M.** (2014). Postsynaptic glutamate receptors regulate local BMP signaling at the Drosophila neuromuscular junction. *Development* **141**, 436–447.

**Tejada-Simon, M. V., Serrano, F., Villasana, L. E., Kanterewicz, B. I., Wu, G. Y., Quinn, M. T. and Klann, E.** (2005). Synaptic localization of a functional NADPH oxidase in the mouse hippocampus. *Molecular and Cellular Neuroscience* **29**, 97–106.

**Thiels, E., Urban, N. N., Gonzalez-Burgos, G. R., Kanterewicz, B. I., Barrionuevo, G., Chu, C. T., Oury, T. D. and Klann, E.** (2000). Impairment of long-term potentiation and associative memory in mice that overexpress extracellular superoxide dismutase. *J Neurosci* **20**, 7631–7639.

**Tirone, F. and Cox, J. A.** (2007). NADPH oxidase 5 (NOX5) interacts with and is regulated by calmodulin. *FEBS Lett* **581**, 1202–1208.

**Tonks, N. K.** (2005). Redox redux: revisiting PTPs and the control of cell signaling. *Cell* **121**, 667–670.

**Tonks, N. K.** (2006). Protein tyrosine phosphatases: from genes, to function, to disease. *Nat Rev Mol Cell Biol* **7**, 833–846.

**Tripodi, M., Evers, J. F., Mauss, A., Bate, M. and Landgraf, M.** (2008). Structural homeostasis: compensatory adjustments of dendritic arbor geometry in response to variations of synaptic input. *PLoS Biol* **6**, e260.

**Tsai, P.-I., Wang, M., Kao, H.-H., Cheng, Y.-J., Lin, Y.-J., Chen, R.-H. and Chien, C.-T.** (2012). Activity-dependent retrograde laminin A signaling regulates synapse growth at Drosophila neuromuscular junctions. *Proc Natl Acad Sci U S A* **109**, 17699–17704.

**Ueda, A. and Wu, C.-F.** (2015). The role of cAMP in synaptic homeostasis in response to environmental temperature challenges and hyperexcitability mutations. *Front Cell Neurosci* **9**, 10.

**Waak, J., Weber, S. S., Görner, K., Schall, C., Ichijo, H., Stehle, T. and Kahle, P. J.** (2009). Oxidizable residues mediating protein stability and cytoprotective interaction of DJ-1 with apoptosis signal-regulating kinase 1. *J Biol Chem* **284**, 14245–14257.

**Wagh, D. A., Rasse, T. M., Asan, E., Hofbauer, A., Schwenkert, I., Dürrbeck, H., Buchner, S., Dabauvalle, M.-C., Schmidt, M. and Qin, G.** (2006). Bruchpilot, a Protein with Homology to

ELKS/CAST, Is Required for Structural Integrity and Function of Synaptic Active Zones in Drosophila. *Neuron* **49**, 833–844.

**Walker, J. A., Gouzi, J. Y., Long, J. B., Huang, S., Maher, R. C., Xia, H., Khalil, K., Ray, A., Van Vactor, D., Bernards, R., et al.** (2013). Genetic and Functional Studies Implicate Synaptic Overgrowth and Ring Gland cAMP/PKA Signaling Defects in the Drosophila melanogaster Neurofibromatosis-1 Growth Deficiency. *PLoS Genet* **9**, e1003958.

**Wang, T., Hauswirth, A. G., Tong, A., Dickman, D. K. and Davis, G. W.** (2014). Endostatin Is a Trans-Synaptic Signal for Homeostatic Synaptic Plasticity. *Neuron*.

**Weyhersmüller, A., Hallermann, S., Wagner, N. and Eilers, J.** (2011). Rapid active zone remodeling during synaptic plasticity. *J Neurosci* **31**, 6041–6052.

**Wilson, C., Muñoz-Palma, E., Henríquez, D. R., Palmisano, I., Núñez, M. T., Di Giovanni, S. and González-Billault, C.** (2016). A Feed-Forward Mechanism Involving the NOX Complex and RyR-Mediated Ca2+ Release During Axonal Specification. *J Neurosci* **36**, 11107–11119.

**Wilson, C., Núñez, M. T. and González-Billault, C.** (2015). Contribution of NADPH oxidase to the establishment of hippocampal neuronal polarity in culture. *J Cell Sci* **128**, 2989–2995.

**Wolfram, V. and Baines, R. A.** (2013). Blurring the boundaries: developmental and activity-dependent determinants of neural circuits. *Trends Neurosci*.

**Yeates, C. J., Zwiefelhofer, D. J. and Frank, C. A.** (2017). The Maintenance of Synaptic Homeostasis at the Drosophila Neuromuscular Junction Is Reversible and Sensitive to High Temperature. *eNeuro* **4**, ENEURO.0220–17.2017.

**Younger, M. A., Müller, M., Tong, A., Pym, E. C. and Davis, G. W.** (2013). A presynaptic ENaC channel drives homeostatic plasticity. *Neuron* **79**, 1183–1196.

**Zhong, Y. and Wu, C.-F.** (2004). Neuronal Activity and Adenylyl Cyclase in Environment-Dependent Plasticity of Axonal Outgrowth in Drosophila. *J Neurosci* **24**, 1439–1445.

**Zhu, X.-H., Qiao, H., Du, F., Xiong, Q., Liu, X., Zhang, X., Ugurbil, K. and Chen, W.** (2012). Quantitative imaging of energy expenditure in human brain. *Neuroimage* **60**, 2107–2117.

**Zwart, M. F., Pulver, S. R., Truman, J. W., Fushiki, A., Fetter, R. D., Cardona, A. and Landgraf, M.** (2016). Selective Inhibition Mediates the Sequential Recruitment of Motor Pools. *Neuron* **91**, 944.

**Zwart, M. F., Randlett, O., Evers, J. F. and Landgraf, M.** (2013). Dendritic growth gated by a steroid hormone receptor underlies increases in activity in the developing Drosophila locomotor system. *Proc Natl Acad Sci U S A*.